count per pixel, and this was used as an index of BM activation in patients before and 1 week after ABMi.

Statistical analysis

Statistical analysis was performed using *t*-test for paired or unpaired samples. Time courses of measurements of liver function parameters were analyzed by repeated-measures ANOVA. A 2-tailed *P* value of <0.05 was considered statistically significant. The data were expressed as mean ± standard error. Analyses were performed using SPSS version 15.0 for Windows (SRSS, Chicago, IL).

Results

Patients characteristics

Five patients received ABMi therapy and were followed up. The baseline demographic features and clinical characteristics of these 5 patients are shown in Table 1. All the patients were men with a mean age of 64 (range: 59–75) years. One patient had ascites, and the other 4 had a history of ascites. All patients had previously undergone endoscopic sclerosing therapy for esophageal varices. CT demonstrated macroscopic cirrhosis with a high degree of liver deformity, and all patients had undergone liver biopsy before the study, which confirmed cirrhosis histologically. The baseline data for the patients who received ABMi in comparison with those for the controls with alcoholic cirrhosis who were matched for age, sex, medication, and liver function parameters are shown in Table 2. There were no significant differences in these baseline data between the 2 groups.

Cell products for ABMi and their characteristics

The characteristics of the cell products for ABMi are shown in Table 3. From 400 mL of autologous BM harvested from the ilium of each patient, the mean number of infused MNCs was $8.0 \pm 7.3 \times 10^9$. The viability of the MNCs was >90% in all cases. The percentages of CD34+, CD44+, CD45+, and CD117+ cells were 6.0% ± 1.8%, 90.1% ± 5.6%, 81.2% ± 6.4%, and 12.0% ± 3.5%, respectively.

Changes in biochemical parameters before and after ABMi

The 5 patients receiving ABMi therapy were followed up for 48 weeks in total: for 24 weeks before and for 24 weeks after ABMi. The 5 controls were also followed up for a total of 48 weeks. Medication was not changed during the study period in any of the patients. The changes of liver function parameters, including serum albumin, total protein, and prothrombin time, are shown in Fig. 1. These parameters all showed an improvement in the patients who received ABMi; the mean level of serum albumin before and 24 weeks after ABMi improved from 3.3 ± 0.2 to 3.8 ± 0.2 g/dL, that of total protein improved from 6.9 ± 0.2 to 7.7 ± 0.1 g/dL, and the prothrombin time improved from 76.6% ± 6.1% to 87.6 % ± 6.0%. The levels of serum albumin, total protein, and prothrombin time during the follow-up period after ABMi were significantly higher than those during the period before ABMi (serum albumin; $P=0.02$, total protein; $P=0.03$, prothrombin time; $P<0.01$). However, no significant changes were observed in the levels of serum albumin and total protein, or prothrombin time, in the controls during the 48 weeks of observation. The Child-Pugh score decreased from 6.8 ± 1.3 before ABMi to 5.8 ± 0.8 at 24 weeks after ABMi. All of the 3 patients who were classified as Child class B with 7 points or higher before ABMi showed a decrease in their scores after ABMi therapy, and the remaining 2 patients classified as Child class A with 6 points or lower showed no change in their scores (Fig. 2).

Changes in liver fibrosis markers

The serum level of the type IV collagen 7S domain was evaluated in patients before and 24 weeks after ABMi. Improvement was observed in 4 of the 5 cases except for case no.5 at 24 weeks after ABMi therapy. The serum levels of the type IV collagen 7S domain decreased from 10.0 ± 3.9 ng/mL before to 8.1 ± 2.3 at 24 weeks after ABMi (Fig. 3), although the change was not significant ($P=0.33$), given the small number of cases examined.

Estimation of liver function using Tc-GSA SPECT

The functional index was improved at 2 weeks in 4 of the 5 patients who received ABMi therapy, and was unchanged in one (case no.1). The mean functional index calculated by Tc-GSA SPECT tended to increase from $2.4 \pm 0.5 \times 10^{-2}$ before ABMi to $2.7 \pm 0.6 \times 10^{-2}$ at 2 weeks after ($P=0.09$) (Fig. 4).

TABLE 1. PATIENT CHARACTERISTICS

							Serum markers					
	Age	*Sex*	*Etiology*	*Ascites*	*Coma*	*Varices*	*T.protein (g/dL)*	*Albumin (g/dL)*	*T.bilirubin (mg/dL)*	*PT (%)*	*ICG R15 (%)(K-ICG)*	*C-P score*
Patient 1	59	M	Alcohol	None (1)[a]	None (1)	positive[b]	6.5	2.7 (3)	1.0 (1)	67 (2)	40 (0.060)	8
Patient 2	61	M	Alcohol	None (1)[a]	None (1)	positive[b]	6.4	2.9 (2)	1.3 (1)	67 (2)	33 (0.077)	7
Patient 3	60	M	Alcohol	None (1)[a]	None (1)	positive[b]	6.7	3.8 (1)	0.8 (1)	92 (1)	27 (0.107)	5
Patient 4	75	M	Alcohol	None (1)[a]	None (1)	positive[b]	7.3	3.3 (2)	2.0 (2)	66 (2)	67 (0.043)	8
Patient 5	69	M	Alcohol	Minimal (2)	None (1)	positive[b]	7.7	3.7 (1)	1.5 (1)	91 (1)	46 (0.073)	6

Number in parentheses indicates points in total Child-Pugh (C-P) score.
[a]History of ascites.
[b]History of endoscopic sclerosing therapy.
T.protein, total protein; T.bilirubin, total bilirubin; PT, prothrombin time activity; ICG-R15, indocyanin green test, retention 15 min.

TABLE 2. BASELINE DATA OF AUTOLOGOUS BONE MARROW INFUSION GROUP AND CONTROL GROUP

Variable	*ABMi group (n=5)*	*Control group (n=5)*	P
Sex (male)	5	5	
Age (years)	64.6±2.9	61.2±4.5	N.S.
Total protein (g/dL)	6.92±0.25	7.22±0.38	N.S.
Serum albumin (g/dL)	3.28±0.22	3.28±0.06	N.S.
Total bilirubin (mg/dL)	1.36±0.20	1.38±0.25	N.S.
Prothrombin time (%)	76.6±6.1	84.8±7.2	N.S.
Medication			
Diuretics	3	3	
BCAA products	4	5	

N.S., not significant (*t*-test). The data are expressed by mean ± standard error.

BCAA, branched chain amino acids; ABMi, autologous bone marrow infusion.

Activated BM distribution assessed by ^{111}In scintigraphy

The ^{111}In count per pixel was increased in 3 of the 4 patients tested at 1 week after ABMi therapy, but was not increased in case no.5. The average ^{111}In count per pixel in these 4 cases increased from 3.7±0.9 before ABMi to 4.4±1.3 at 1 week after (Fig. 5A), although the changes were not significant ($P=0.23$), given the small number of cases. The BM image in case no. 2, with the highest increase in the ^{111}In count after ABMi therapy, is shown in Fig. 5B. Activation of BM cells in case no.2 was demonstrated by an increase in the ^{111}In count per pixel from 4.5 before to 6.3 at 1 week after ABMi.

Complications

None of the 5 patients who received ABMi therapy exhibited any serious complications during or after the procedure.

Discussion

This study showed that ABMi for patients with ALC could be performed safely under general anesthesia and that it improved their liver function parameters including the serum levels of albumin and total protein and the prothrombin time. The Child-Pugh score also improved in all 3 patients who had a score higher than 7, which was classified as class B. Further, ABMi resulted in induction of hepatic functional reserve, as suggested by Tc-GSA SPECT imaging as well as reduction of the serum levels of the fibrosis marker in 4 of the 5 cases examined.

It is generally accepted that the results of laboratory tests can be modified by drug administration or infusion of albumin products or plasma. Although both patients treated with ABMi and controls had received several types of medication, the administered drugs were not changed during the study period, whereas the patients abstained from alcohol and no blood products were supplied. Abstinence is an important factor to consider when selecting patients for ABMi, because ALC is an irreversible liver condition resulting from chronic inflammation attributable to the toxic effect of ethanol on the liver. For enrollment in the present study, patients who showed marked deformity of the liver on CT, and histologically proved cirrhosis, were required to have abstained from alcohol for at least 24 weeks. No changes in liver function parameters were found as a result of an abstinence in either the controls or the patients treated with ABMi in the period before ABMi. However, the results of the present study suggest that liver function parameters can be improved by ABMi in patients with ALC. A recent study has shown that patients who undergo orthotropic liver transplantation for alcoholic liver disease have a rate of recidivism as high as 28% at 9 years [21]. Therefore, both careful observation and adequate intervention in relation to abstinence may be required for patients after ABMi.

Although BM stem cell treatment for liver cirrhosis is an attractive strategy in the field of liver regenerative cell therapy, many concerns need to be addressed [22,23]. It is still unclear how infused BM cells work for the improvement of liver function. We have demonstrated experimentally that BM cells transplanted into the spleen of rats with liver damage induced by carbon tetrachloride express liver-specific proteins such as alpha-fetoprotein in their cytoplasm in the recipient liver [10]. A clinical trial of ABMi for patients with cirrhosis has also demonstrated that the number of alpha-fetoprotein-positive cells was increased significantly in the liver, relative to the situation before ABMi. In addition, ABMi appeared to induce hepatocyte proliferation in the liver, as expression of proliferating cell nuclear antigen, a marker of hepatocyte proliferation, was significantly increased after ABMi in comparison with the pretreatment situation [15]. Another study has shown that intraportal administration of autologous CD133+ BM cells and subsequent portal venous embolization of right liver segments resulted in a 2.5-fold increase in the mean proliferation rate of the left lateral segment, in comparison with controls not

TABLE 3. CHARACTERISTICS OF PROCESSED MONONUCLEAR CELLS

	Harvest vol. (mL)	*No. of infused MNCs (X 10^9)*	*CD34+ (%)*	*CD44+ (%)*	*CD45+ (%)*	*CD117+ (%)*
Patient 1	400	3.0	4.3	87.7	85.2	10.9
Patient 2	400	2.5	8.8	84.4	78.8	15.9
Patient 3	400	16.0	5.2	93.7	82.4	8.2
Patient 4	400	2.3	5.2	97.9	88.0	15.5
Patient 5	400	16.0	6.7	86.6	71.4	9.6
Mean±SE		8.0±7.3	6.0±1.8	90.1±5.6	81.2±6.4	12.0±3.5

MNC, mononuclear cell.

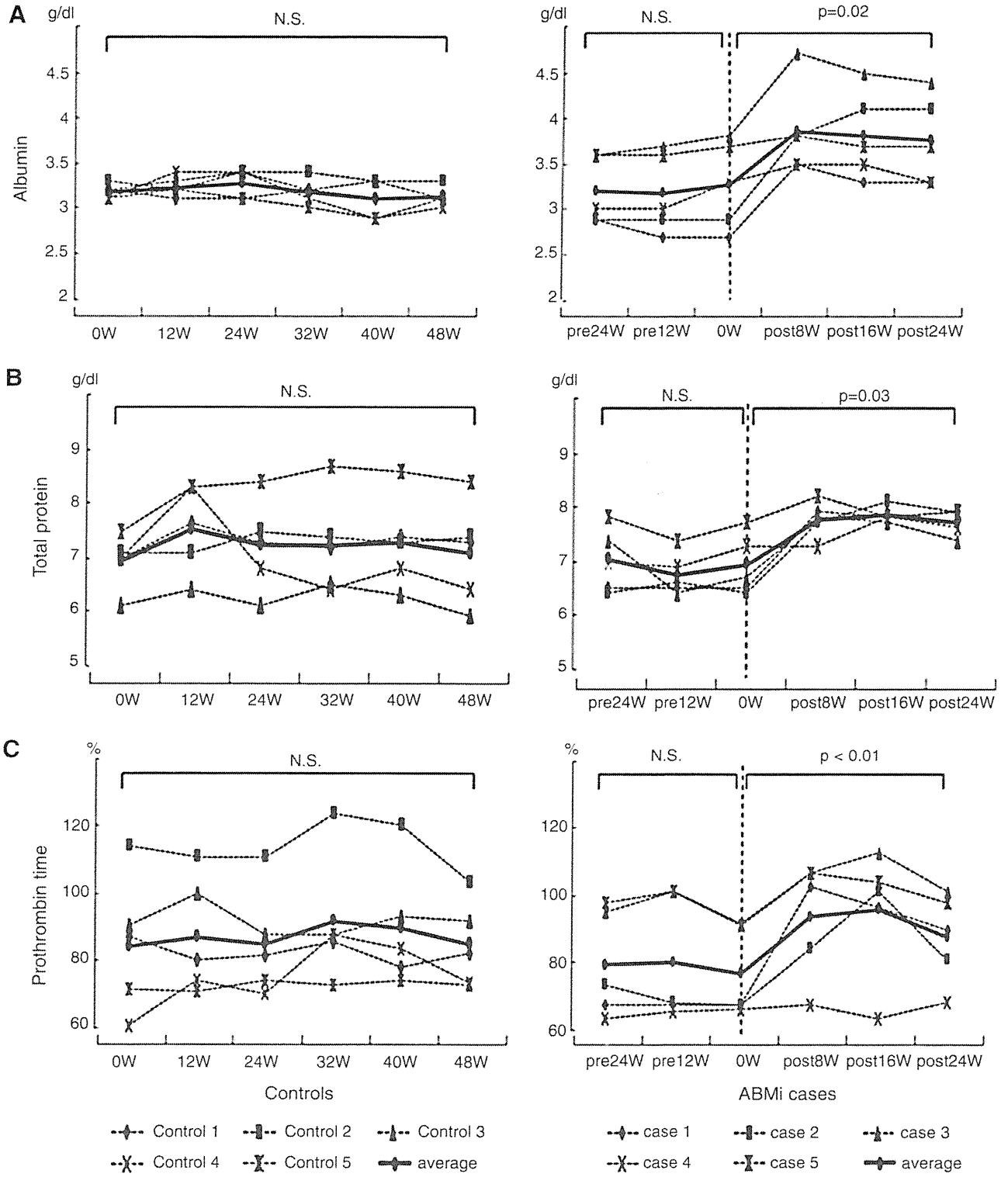

FIG. 1. Changes in biochemical parameters before and after ABMi. The levels of serum albumin (A) and total protein (B), and prothrombin time (C), during the follow-up of patients after ABMi were significantly higher than those during the period before ABMi. No significant changes were observed in the controls. ABMi, autologous bone marrow infusion.

receiving BM transfusion [24]. These data suggest that transplanted BM cells have a potential role in liver regeneration and proliferate in the recipient liver and that this process is likely to occur early after ABMi, as Tc-GSA SPECT analysis in the present study demonstrated an increase in the liver function index of most patients 2 weeks after ABMi. However, since it is still unclear whether fully functional hepatocytes are induced by ABMi, the characteristics of BM

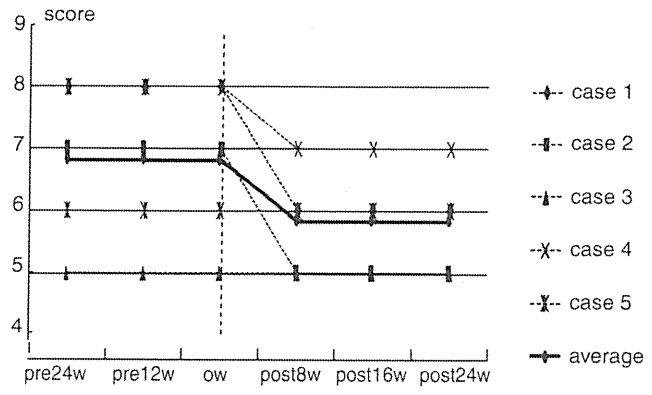

FIG. 2. Changes in Child-Pugh score after ABMi in comparison with those before. The Child-Pugh score decreased from 6.8±1.3 before ABMi to 5.8±0.8 at 24 weeks after ABMi. All of the 3 patients classified as class B, scoring 7 points or higher before ABMi, showed a decrease in their scores after the therapy.

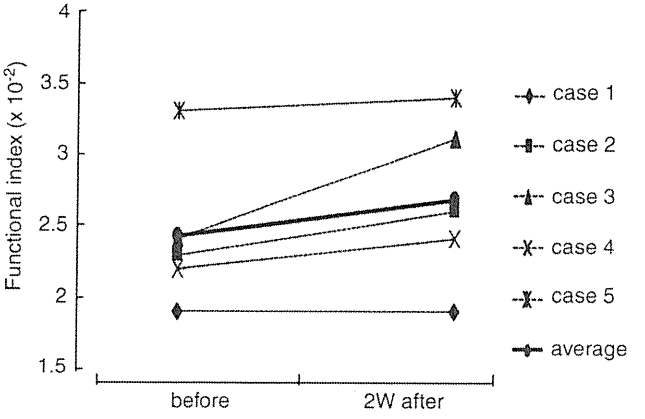

FIG. 4. Estimation of liver function using technetium 99m galactosyl-human serum albumin single photon emission computed tomography. The functional index improved in 4 of the 5 cases, and did not change in one (case 1) after ABMi. The mean functional index tended to increase from $2.4\pm0.5\times10^{-2}$ before ABMi to $2.7\pm0.6\times10^{-2}$ at 2 weeks after ($P=0.09$).

stem cells that show hepatocyte differentiation should be elucidated further. In addition, to elucidate the cell-cell communication in the extracellular microenvironment that would be important for tissue repair, many markers originating from the different cell types among MNCs should be investigated in the future.

The tracking of BM cells infused into the human body as a means of monitoring cell engraftment after ABMi has not been previously reported. In the present study, BM scintigraphy using ^{111}In before and after ABMi showed that the distribution of activated BM was enhanced systemically after ABMi, including the liver, in 3 of the 4 patients examined. Although the process of migration of infused BM cells to the liver remains unknown, clarification of the factors responsible could yield important data for improving the efficiency of transplantation. In fact, ABMi case no. 2, in which the greatest increase in the ^{111}In count was observed 1 week after ABMi, showed a marked decrease in the concentration of the

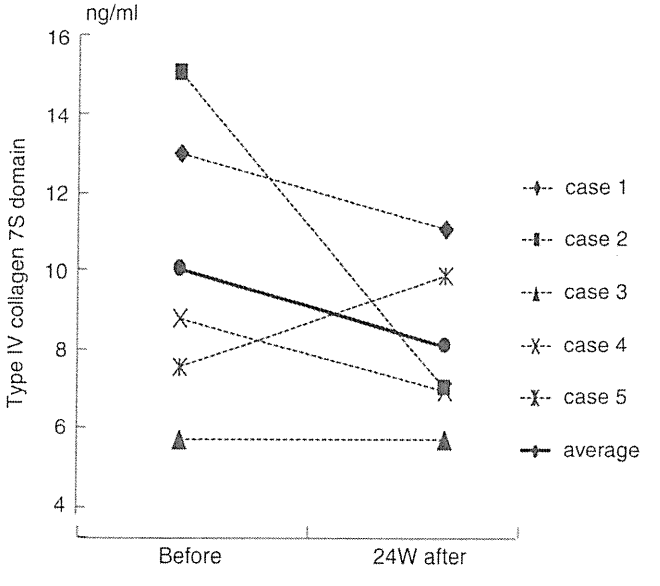

FIG. 3. Changes in the levels of a liver fibrosis marker after ABMi in comparison with those before. The level of the type IV collagen 7S domain improved in 4 of the 5 cases, with the exception of case no.5, at 24 weeks after ABMi therapy, and their serum levels decreased from 10.0±3.9 ng/mL before to 8.1±2.3 ng/mL at 24 weeks after the therapy.

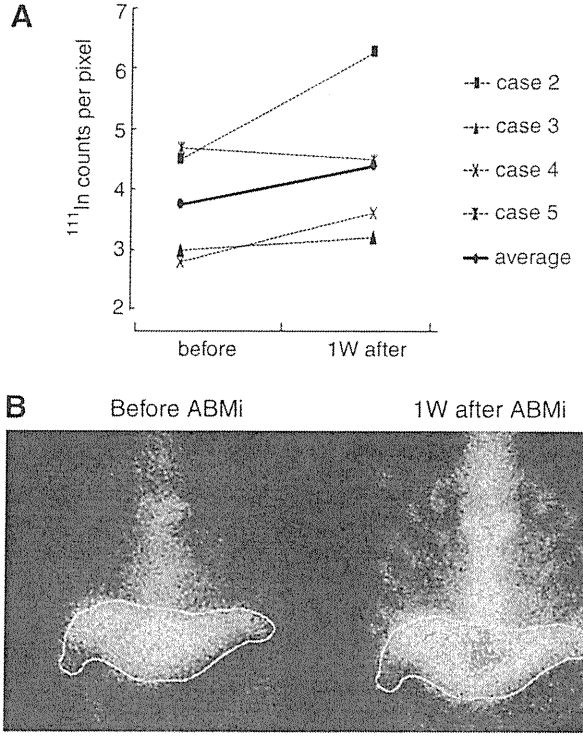

FIG. 5. Activated BM distribution demonstrated by indium-111-chloride (^{111}In) scintigraphy. **(A)** The ^{111}In count per pixel increased in 3 of the 4 patients tested after ABMi therapy, with the exception of case no.5. The average ^{111}In count per pixel in the 4 patients increased from 3.7±0.9 before to 4.4±1.3 after ABMi. **(B)** BM image of case no. 2, showing the greatest increase of the ^{111}In count 1 week after ABMi therapy (4.5 before to 6.3 after).

type IV collagen 7S domain, as shown in Fig. 3, as well as a marked improvement of liver function parameters, as shown in Fig. 1. In contrast, ABMi case no.5 was only one showing no change in the ^{111}In count at 1 week after ABMi, and the only case in which the level of the type IV collagen 7S domain did not decrease after ABMi. Effective migration of infused BM cells to the liver may ameliorate liver fibrosis, because such cells have been shown experimentally to produce and secrete anti-fibrosis factors such as matrix metalloproteinase-9 [7]. At this time, the factors that determine the difference between effectiveness and noneffectiveness are unclear. Collateral circulation resulting from the portal vein disorganization that characterizes liver cirrhosis may affect the flow and effective migration of infused BM cells to the liver, and, thus, migration of infused cells to the liver may partly depend on the portal venous pressure. Further, the expression levels of cellular adhesion molecules associated with the attachment of infused cells to liver tissue may vary a great deal among patients. It is important to determine the adhesion molecules that are induced in the liver tissue of patients receiving ABMi. Further studies are needed to clarify the mechanisms involved in the migration of infused BM cells to the liver.

The present study did not demonstrate the long-term effectiveness of this therapy in terms of survival rate or improvement in the quality of life. Such effects will need to be evaluated by a randomized controlled study in the future. In addition, improvements in the methods of delivering infused BM cells to the human body should also be investigated further. We are currently conducting experiments aimed at improving the effectiveness of this therapy by investigating the long-term culture conditions for BM cells, the optimum cell population to be employed, the effectiveness of repeated transplantation of BMCs, and the optimum route of cell delivery. We have already confirmed both the safety and short-term efficacy of ABMi therapy for various liver diseases [15,16], and these basic data are expected to be of value for improving ABMi therapy in the near future.

In summary, ABMi therapy for patients with alcoholic cirrhosis has been shown to improve liver function parameters, in contrast to observation accompanied by abstinence from alcohol. The markers of liver fibrosis, hepatic functional reserve, and BM cell activation were improved in most of the patients who received ABMi therapy. However, the degree of effectiveness of ABMi is likely to differ among patients, and the present results should still be considered in terms of a pilot study. Further investigation of factors associated with the effectiveness of this therapy is warranted, and future studies will need to assess the safety of this therapy and its effect on liver function in a large number of patients, together with its long-term effectiveness, in terms of survival rate and quality of life.

Acknowledgments

This study was supported in part by a grant from the Ministry of Health, Labor, and Welfare of Japan, and also in part by a Grant-in-Aid from the Global COE program of the Japan Society for the Promotion of Science. The authors thank Dr. K. Okita for his support toward this study.

Author Disclosure Statement

The authors declare that they have no conflict of interest.

References

1. Krause K, C Schneider, KH Kuck and K Jaquet. (2010). Stem cell therapy in cardiovascular disorders. Cardiovasc Ther 28:e101–e110.
2. Bui QT, ZM Gertz and RL Wilensky. (2010). Intracoronary delivery of bone-marrow-derived stem cells. Stem Cell Res Ther 1:29.
3. Petersen BE, WC Bowen, KD Patrene, WM Mars, AK Sullivan, N Murase, SS Boggs, JS Greenberger and JP Goff. (1999). Bone marrow as a potential source of hepatic oval cells. Science 284:1168–1170.
4. Alison MR, R Poulsom, R Jeffery, AP Dhillon, A Quaglia, J Jacob, M Novelli, G Prentice, J Williamson and NA Wright. (2000). Hepatocytes from non-hepatic adult stem cells. Nature 406:257.
5. Theise ND, S Badve, R Saxena, O Henegariu, S Sell, JM Crawford and DS Krause. (2000). Derivation of hepatocytes from bone marrow cells in mice after radiation-induced myeloablation. Hepatology 31:235–240.
6. Theise ND, M Nimmakayalu, R Gardner, PB Illei, G Morgan, L Teperman, O Henegariu and DS Krause. (2000). Liver from bone marrow in humans. Hepatology 32:11–16.
7. Sakaida I, S Terai, N Yamamoto, K Aoyama, T Ishikawa, H Nishina and K Okita. (2004). Transplantation of bone marrow cells reduces CCl4-induced liver fibrosis in mice. Hepatology 40:1304–1311.
8. Terai S, I Sakaida, N Yamamoto, K Omori, T Watanabe, S Ohata, T Katada, K Miyamoto, K Shinoda, H Nishina and K Okita. (2003). An in vivo model for monitoring transdifferentiation of bone marrow cells into functional hepatocytes. J Biochem 134:551–558.
9. Okumoto K, T Saito, E Hattori, JI Ito, A Suzuki, K Misawa, R Ishii, T Karasawa, H Haga, M Sanjo, T Takeda, K Sugahara, K Saito, H Togashi and S Kawata. (2005). Differentiation of rat bone marrow cells cultured on artificial basement membrane containing extracellular matrix into a liver cell lineage. J Hepatol 43:110–116.
10. Okumoto K, T Saito, E Hattori, JI Ito, A Suzuki, K Misawa, M Sanjyo, T Takeda, K Sugahara, K Saito, H Togashi and S Kawata. (2005). Expression of Notch signaling markers in bone marrow cells that differentiate into a liver cell lineage in a rat transplanted model. Hepatol Res 31:7–12.
11. Okumoto K, T Saito, H Haga, E Hattori, R Ishii, T Karasawa, A Suzuki, K Misawa, M Sanjo, JI Ito, K Sugahara, K Saito, H Togashi and S Kawata. (2006). Characteristics of rat bone marrow cells differentiated into a liver cell lineage and dynamics of the transplanted cells in the injured liver. J Gastroenterol 41:62–69.
12. Haga H, T Saito, K Okumoto, S Ugajin, C Sato, R Ishii, Y Nishise, J Ito, H Watanabe, K Saito, H Togashi and S Kawata. (2011). Enhanced expression of fibroblast growth factor 2 in bone marrow cells and its potential role in the differentiation of hepatic epithelial stem-like cells into hepatocyte lineage. Cell Tissue Res 343:371–378.
13. Gordon MY, N Levicar, M Pai, P Bachellier, I Dimarakis, F Al-Allaf, H M'Hamdi, T Thalji, JP Welsh, SB Marley, J Davies, F Dazzi, F Marelli-Berg, P Tait, R Playford, L Jiao, S Jensen, JP Nicholls, A Ayav, M Nohandani, F Farzaneh, J Gaken, R Dodge, M Alison, JF Apperley, R Lechler and NA Habib. (2006). Characterization and clinical application of human CD34+ stem/progenitor cell populations mobilized into the blood by granulocyte colony-stimulating factor. Stem Cells 24:1822–1830.

14. Levicar N, M Pai, NA Habib, P Tait, LR Jiao, SB Marley, J Davis, F Dazzi, C Smadja, SL Jensen, JP Nicholls, JF Apperley and MY Gordon. (2008). Long-term clinical results of autologous infusion of mobilized adult bone marrow derived CD34+ cells in patients with chronic liver disease. Cell Prolif 41 (Suppl 1):115–125.
15. Terai S, T Ishikawa, K Omori, K Aoyama, Y Marumoto, Y Urata, Y Yokoyama, K Uchida, T Yamasaki, Y Fujii, K Okita and I Sakaida. (2006). Improved liver function in patients with liver cirrhosis after autologous bone marrow cell infusion therapy. Stem Cells 24:2292–2298.
16. Kim JK, YN Park, JS Kim, MS Park, YH Paik, JY Seok, YE Chung, HO Kim, KS Kim, SH Ahn, DY Kim, MJ Kim, KS Lee, CY Chon, SJ Kim, S Terai, I Sakaida and KH Han. (2010). Autologous bone marrow infusion activates the progenitor cell compartment in patients with advanced liver cirrhosis. Cell Transplant 19:1237–1246.
17. Pai M, D Zacharoulis, MN Milicevic, S Helmy, LR Jiao, N Levicar, P Tait, M Scott, SB Marley, K Jestice, M Glibetic, D Bansi, SA Khan, D Kyriakou, C Rountas, A Thillainayagam, JP Nicholls, S Jensen, JF Apperley, MY Gordon and NA Habib. (2008). Autologous infusion of expanded mobilized adult bone marrow-derived CD34+ cells into patients with alcoholic liver cirrhosis. Am J Gastroenterol 103:1952–1958.
18. Sugahara K, H Togashi, K Takahashi, Y Onodera, M Sanjo, K Misawa, A Suzuki, T Adachi, J Ito, K Okumoto, E Hattori, T Takeda, H Watanabe, K Saito, T Saito, Y Sugai and S Kawata. (2003). Separate analysis of asialoglycoprotein receptors in the right and left hepatic lobes using Tc-GSA SPECT. Hepatology 38:1401–1409.
19. Kudo M, A Todo, K Ikekubo, K Yamamoto, DR Vera and RC Stadalnik. (1993). Quantitative assessment of hepatocellular function through in vivo radioreceptor imaging with technetium 99m galactosyl human serum albumin. Hepatology 17:814–819.
20. Kwon AH, SK Ha-Kawa, S Uetsuji, Y Kamiyama and Y Tanaka. (1995). Use of technetium 99m diethylenetriaminepentaacetic acid-galactosyl-human serum albumin liver scintigraphy in the evaluation of preoperative and postoperative hepatic functional reserve for hepatectomy. Surgery 117:429–434.
21. Biselli M, A Gramenzi, M Del Gaudio, M Ravaioli, G Vitale, S Gitto, GL Grazi, AD Pinna, P Andreone and M Bernardi; Bologna Liver Transplantation Group. (2010). Long term follow-up and outcome of liver transplantation for alcoholic liver disease: a single center case-control study. Clin Gastroenterol 44:52–57.
22. Kallis YN, MR Alison and SJ Forbes. (2007). Bone marrow stem cells and liver disease. Gut 56:716–724.
23. Lorenzini S and P Andreone. (2007). Stem cell therapy for human liver cirrhosis: a cautious analysis of the results. Stem Cells 25:2383–2384.
24. am Esch JS 2nd, WT Knoefel, M Klein, A Ghodsizad, G Fuerst, LW Poll, C Piechaczek, ER Burchardt, N Feifel, V Stoldt, M Stockschläder, N Stoecklein, RY Tustas, CF Eisenberger, M Peiper, D Häussinger and SB Hosch. (2005). Portal application of autologous CD133+ bone marrow cells to the liver: a novel concept to support hepatic regeneration. Stem Cells 23:463–470.

Address correspondence to:
Dr. Takafumi Saito
Department of Gastroenterology
Yamagata University School of Medicine
2-2-2 Iida-nishi
Yamagata 990-9585
Japan

E-mail: tasaitoh@med.id.yamagata-u.ac.jp

Received for publication February 16, 2011
Accepted after revision March 20, 2011
Prepublished on Liebert Instant Online March 20, 2011

Ann Nucl Med (2011) 25:520–523
DOI 10.1007/s12149-011-0484-0

CASE REPORT

^{99m}Tc-GSA SPECT analysis was clinically useful to evaluate the effect of interferon in a patient with interferon non-responsive chronic hepatitis C

Rika Ishii · Hitoshi Togashi · Akiko Iwaba · Chikako Sato · Hiroaki Haga · Mai Sanjo · Kazuo Okumoto · Yuko Nishise · Jun-itsu Ito · Hisayoshi Watanabe · Koji Saito · Akio Okada · Kazuei Takahashi · Takafumi Saito · Sumio Kawata

Received: 15 December 2010 / Accepted: 23 February 2011 / Published online: 2 April 2011

Abstract We describe a 62-year-old woman with advanced chronic hepatitis C who showed no response to low-dose long-term interferon-beta monotherapy (3 MU, three times a week). The interferon monotherapy was continued for 2 years and 9 months. Despite this lack of response to interferon, the patient's clinical course was good and liver function assessed by ^{99m}Tc-galactosyl human serum albumin single photon emission computed tomography (^{99m}Tc-GSA SPECT) analysis improved significantly. Improvement of the data obtained by ^{99m}Tc-GSA SPECT analysis justified continuation of the treatment. ^{99m}Tc-GSA SPECT analysis was clinically useful to evaluate the effect of interferon in a patient with interferon non-responsive chronic hepatitis C, despite a lack of reduction of the ALT level and HCV-RNA titer.

Keywords Chronic hepatitis C · Interferon non-responder · ^{99m}Tc-GSA SPECT

R. Ishii · H. Togashi · C. Sato · H. Haga · M. Sanjo · K. Okumoto · Y. Nishise · J. Ito · H. Watanabe · K. Saito · T. Saito · S. Kawata
Department of Gastroenterology, Yamagata University Faculty of Medicine, 2-2-2 Iida-nishi, Yamagata 990-9585, Japan

H. Togashi (✉)
Yamagata University Health Administration Center, 1-4-12 Kojirakawa-machi, Yamagata 990-8560, Japan
e-mail: htogashi@med.id.yamagata-u.ac.jp

A. Iwaba
Department of Pathological Diagnostics, Yamagata University Faculty of Medicine, 2-2-2 Iida-nishi, Yamagata 990-9585, Japan

A. Okada · K. Takahashi
Department of Radiology, Yamagata University Faculty of Medicine, 2-2-2 Iida-nishi, Yamagata 990-9585, Japan

Introduction

Hepatitis C virus (HCV) usually causes chronic infection, which can result in chronic hepatitis, liver cirrhosis, and hepatocellular carcinoma over the course of several decades [1]. However, effective treatment is available. Interferon (IFN) is able to eradicate HCV and can induce marked biochemical and histological improvement [2]. The current standard therapy for chronic HCV infection is a combination of pegylated IFN and ribavirin [3]. In patients with high viral loads of genotype 1, the rate of sustained virological response is about 50% for this combination treatment. However, patients who do not respond, or in whom the treatment fails because of severe complications, are referred for new treatment options. Although low-dose long-term interferon (IFN maintenance) therapy has been attempted as a new treatment option, its efficacy in terms of liver function and histology has varied markedly among previous reports [4–7]. The real-time evaluation of IFN therapy in patients with chronic hepatitis C who are truly IFN-non-responsive during the therapy will help in justifying the validity of continuation of IFN therapy.

The asialoglycoprotein receptor (ASGPR) is abundantly expressed on the sinusoidal surface of the hepatocytes adjacent to the extracellular space of Disse in the liver. It is tempting to speculate that the ASGPR may be a relevant factor in the inflammation and fibrosis associated with chronic viral hepatitis. We have developed ^{99m}Tc-GSA SPECT analysis that can evaluate regional hepatic function and the progression of chronic viral hepatitis using dynamic changes in ASGPRs [8]. Here, we report a patient with chronic hepatitis C who received interferon-beta (IFN-β) maintenance therapy, and whose liver function and histology improved significantly, even though the ALT level was not controllable and the viral load did not

decrease during the therapy. Improvement of the data obtained by ^{99m}Tc-GSA SPECT analysis justified continuation of the treatment.

Case report

A 62-year-old woman was admitted to our hospital for further examination of liver dysfunction on April 10, 2002. Liver biochemical tests showed elevated levels of aspartate aminotransferase (AST 69 IU/l) and alanine aminotransferase (ALT 68 IU/l). The patient was seronegative for all hepatitis B virus markers, but seropositive for anti-HCV by a third-generation enzyme immunoassay. The HCV-RNA titer was high (>850 KIU/ml) and the genotype was 1b (Table 1). Liver biopsy was performed on April 12, 2002, and this demonstrated severe fibrosis and moderate inflammation activity in portal areas (Fig. 1a, b). On April 16, 2002, ^{99m}Tc-GSA SPECT was performed, and this indicated that liver uptake ratio (LUR) and liver uptake density (LUD) of the whole liver were 74 and 0.048%/ml, respectively. The patient had no history of excessive alcohol intake, and was diagnosed as having advanced chronic hepatitis C. In 1995, she received natural IFN-α monotherapy in other hospital, but the monotherapy was withdrawn after 3 months because of non-response and adverse effects. When considering the therapeutic history, we planned to treat the patient with recombinant interferon alpha-2b (IFN-α2b: Intron A, Schering-Plough, Kenilworth, NJ), 6 MU daily for 2 weeks, and then three times a week for an additional 22 weeks in combination with peroral ribavirin at 600 mg/day [Revetol, Schering-Plough (RBV)]. From April 22, 2002, 6 MU of IFN-α2b combined with 600 mg/day RBV was started. The combination therapy was continued, by adjusting the dosage of IFN-α2b and RBV in accordance with any adverse effects, such as leukocytopenia and thrombocytopenia. However, as the patient was non-responsive to the recombinant IFN-α2b and RBV combination therapy, it was withdrawn on November 25, 2002 (Fig. 2).

Table 1 Laboratory data at first admission

WBC	3,670/μl	TP	7.4 g/dl	FBS	83 mg/dl
RBC	4.07×10^6	ALB	4.4 g/dl	T-Cho	174 mg/dl
Hb	13.4 g/dl	ZTT	8.7 IU/l	TG	91 mg/dl
Ht	39.9%	T-BIL	0.6 mg/dl	AFP	7.4 ng/ml
Plt	11.0×10^3/μl	D-BIL	0.2 mg/dl		
PT	132.4%	AST	69 IU/l	HBsAg	(−)
Na	146 mEq/l	ALT	68 IU/l	HCV-Ab	(+)
K	4.4 mEq/l	LDH	412 IU/l	HCV-RNA	>850 KIU/ml
Cl	105 mEq/l	ALP	87 IU/l	HCV genotype	1b
BUN	14 mg/dl	γ-GTP	28 IU/l		
CREA	0.7 mg/dl	ChE	411 IU/l		
UA	4.6 mg/dl				

AFP alpha-fetoprotein, *ALB* albumin, *ALP* alkaline phosphatase, *ALT* alanine aminotransferase, *AST* aspartate aminotransferase, *BUN* blood urea nitrogen, *ChE* cholinesterase, *Cl* chloride, *CREA* creatine, *D-Bil* direct bilirubin, *γ-GTP* gamma glutamyl transpeptidase, *Hb* hemoglobin, *HBsAg* hepatitis B virus surface antigen, *HCV-Ab* hepatitis C virus antibody, *HCV-RNA* hepatitis C virus RNA, *Ht* hematocrit, *K* potassium, *LDH* lactate dehydrogenase, *Na* sodium, *Plt* platelets, *PT* prothrombin time, *RBC* red blood cells, *T-Bil* total bilirubin, *T-Chol* total cholesterol, *TG* triglyceride, *TP* total protein, *UA* uric acid, *WBC* white blood cells, *ZTT* zinc sulfate turbidity test

We previously reported that ^{99m}Tc-GSA SPECT analysis was clinically useful in evaluating regional hepatic function and the progression of chronic viral hepatitis using dynamic changes in the asialoglycoprotein receptors [8]. On April 13, 2004, ^{99m}Tc-GSA SPECT analysis was performed, and the indices obtained, LUR and LUD, which reflect the amount and density of asialoglycoprotein receptors in the liver, respectively, were found to be decreased considerably during the 2 years' follow-up period (Fig. 1c). The LUR correlated particularly well with conventional liver function tests, and LUD was a good indicator of periportal and/or bridging necrosis and fibrosis [8]. The patient was diagnosed as having advanced chronic hepatitis.

On July 1, 2004, 3 MU of IFN-β (IFN-β: Toray Co., Tokyo), three times a week, was administered intravenously to improve the function of the liver, as the ALT level remained at more than 50 IU/l and the patient strongly desired IFN maintenance therapy. IFN-β was used because of fewer side effects when compared with IFN-α. The written informed consent was obtained before the start of the IFN-β therapy. In contrast to our expectation, however, the ALT level did not decrease after induction of the IFN-β maintenance therapy, and remained at over 50 IU/l. Moreover, the HCV-RNA titer increased. The IFN-β maintenance therapy was continued because the patient had no serious complications, and compliance was satisfactory. On March 10, 2005, ^{99m}Tc-GSA SPECT analysis was performed again, and this indicated that LUR and LUD of the whole liver were 74 and 0.046%/ml, respectively, suggesting a significant improvement. On March 30, 2007, IFN-β maintenance therapy was completed after a total duration of 2 years and 9 months (Fig. 2).

Thereafter, ALT gradually decreased (Fig. 2). Repeat ^{99m}Tc-GSA SPECT analysis at 1 year after the completion of INF-β maintenance therapy indicated further improvement of LUR and LUD (Fig. 3a). The LUR and the LUD values for whole liver and right lobes recovered to the mean values for normal control group. Liver biopsy was also conducted 1 year after the completion of IFN-β maintenance therapy (October 1, 2008), and the histology showed significant improvement of hepatic fibrosis and diminished portal inflammation (Fig. 3b, c). Throughout

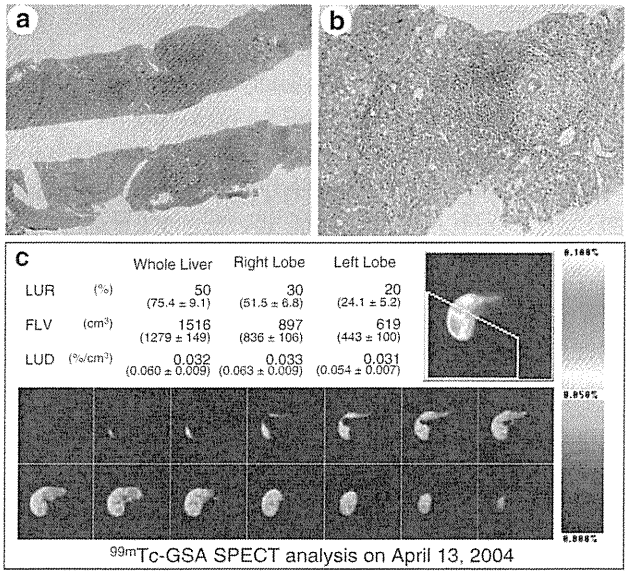

Fig. 1 Histopathology and ^{99m}Tc-GSA SPECT analysis. **a** and **b** Histopathology of the liver on April 12, 2002. Severe hepatic fibrosis and moderate inflammatory activity in the portal areas are evident. **a** Elastica–Masson staining, ×4 magnification with objective lens. **b** H&E staining, ×20 magnification with objective lens. **c** Images and data from ^{99m}Tc-GSA SPECT analysis conducted on April 13, 2004. A decrease in the liver uptake ratio of ^{99m}Tc-GSA and the expression of ASGPRs was demonstrated. Mean and standard values for normal control group are indicated in *parentheses*. The patient was diagnosed as having advanced chronic hepatitis

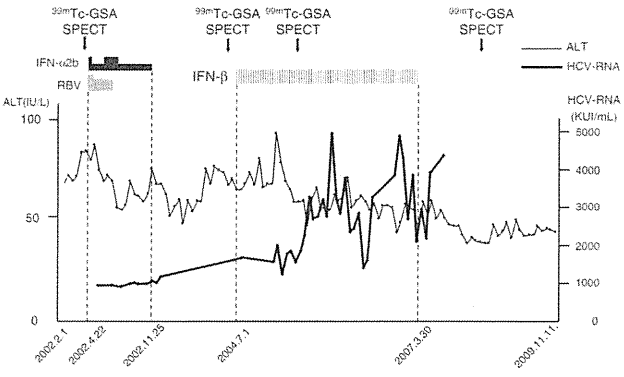

Fig. 2 Clinical course of the patient. On April 22, 2002, recombinant IFN-α2b and RBV combination therapy was started by adjusting the dosage of IFN-α2b and RBV in accordance with adverse effects. The therapy was continued until November 25, 2002. The patient was non-responsive to the combination therapy. Because the ALT level remained high (>60 IU/l), we introduced IFN-β maintenance therapy, but the ALT level and HCV-RNA titer did not decrease at all. However, ^{99m}Tc-GSA SPECT analysis performed on March 10, 2005, showed a significant improvement of hepatic functional reserve. IFN-β maintenance therapy was continued for a total of 2 years and 9 months. After completion of the therapy, the ALT level gradually decreased and the patient's condition has been good up to the time of writing

the clinical course, she was administered ursodeoxycholic acid (300 mg/day per orally), but was not administered angiotensin-converting enzyme inhibitors, AT1-receptor

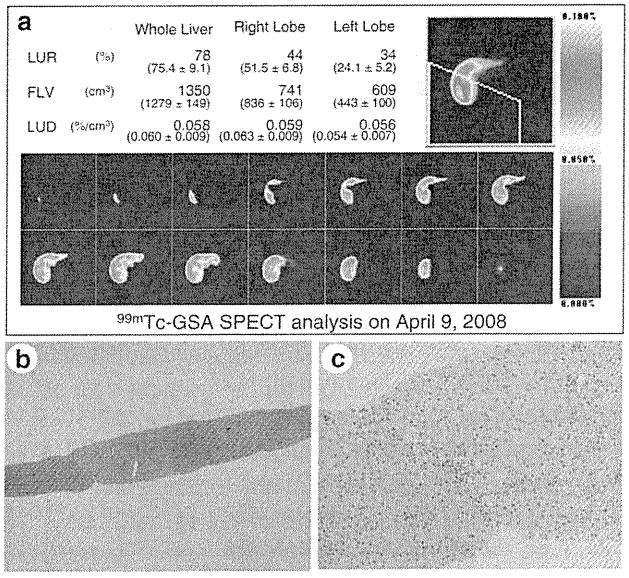

Fig. 3 ^{99m}Tc-GSA SPECT analysis and histopathology. **a** Images and data from ^{99m}Tc-GSA SPECT analysis conducted on April 9, 2008. After 1 year of completion of IFN-β monotherapy, ^{99m}Tc-GSA SPECT indicated an increase in LUR and LUD in comparison with the data obtained on March 10, 2005 and April 13, 2004 (Fig. 1c), indicating a significant improvement of liver function. **b**, **c** Histopathology of a liver biopsy obtained on October 1, 2008. One year and 7 months after the completion of IFN-β monotherapy, the histopathology showed a decrease of hepatic fibrosis and diminished hepatic inflammation, suggesting a significant improvement. **b** Elastica–Masson staining, ×4 magnification with objective lens. **c** H&E staining, ×20 magnification with objective lens

blockers, nor glycyrrhizin injection. The patient's clinical course has since remained favorable, and the ALT level has been controllable with no sign of hepatocellular carcinoma up to the time of writing.

Discussion

The present case of chronic hepatitis C showed resistance to previously performed IFN-α2b and ribavirin combination therapy. As a new option for this difficult-to-treat patient, we administered 3 MU of IFN-β three times per week intravenously. After IFN-β induction, there was no decline of transaminase levels, and the HCV-RNA titer increased somewhat. Because there were no adverse complications and the patient's compliance was satisfactory, we continued the maintenance therapy for a further 2 years and 9 months, anticipating that the IFN-β would have an anti-fibrotic effect [9], in parallel with the confirmation of liver function by ^{99m}Tc-GSA SPECT analysis. Even after withdrawal of the maintenance IFN-β therapy, the patient's condition has been good, and the results of ^{99m}Tc-GSA SPECT analysis and liver biopsy histology have improved considerably.

The Japanese Guidelines for the treatment of chronic hepatitis C recommend low-dose interferon monotherapy when the ALT level is controllable by the treatment [10]. Shiffman et al. [4] reported that a reduction in the HCV-RNA titer could be used to predict which patients would achieve a histological response and could be potential candidates for maintenance interferon therapy. In the present case, however, although there was no decrease in the ALT level or HCV-RNA titer, liver function improved gradually as a result of the IFN-β maintenance therapy. To access the justification of continuation of IFN therapy, we have adopted ^{99m}Tc-GSA SPECT analysis that can readily be performed and allows evaluation of hepatic functional reserve and the degree of hepatic inflammation and fibrosis. Improvement of the data obtained by ^{99m}Tc-GSA SPECT analysis justified continuation of the treatment. ^{99m}Tc-GSA SPECT analysis is clinically useful for patients with this condition.

IFN-α and -β are both used for the treatment of chronic hepatitis C. Both recognize common interferon receptors, and express IFN activity. IFN-α and -β are well known to have an anti-fibrotic effect in damaged liver [9, 11]. IFN-β has higher affinity for the IFN receptor than IFN-α and consequently shows stronger induction of IFN-regulated genes [12]. One explanatory hypothesis for the anti-fibrotic effect is that IFN-β strongly reduces the expression of mRNAs for transforming growth factor-β, basic fibroblast growth factor, collagen type I A2 and tissue inhibitor of metalloproteinase I, which are related to the progression of liver fibrosis [9]. Another plausible hypothesis may be that IFN-β enhances the expression of interleukin 10 [13], which had been reported to decrease disease activity in chronic hepatitis C patients [14]. We thus considered that IFN-β might be beneficial for some patients who were resistant to IFN-α.

In conclusion, the present case was considered to offer important information that ^{99m}Tc-GSA SPECT analysis was helpful in justifying continuation of IFN therapy for IFN-non-responsive chronic hepatitis C without frequent liver biopsy.

References

1. Ikeda K, Saitoh S, Suzuki Y, Kobayashi M, Tsubota A, Koida I, et al. Disease progression and hepatocellular carcinogenesis in patients with chronic viral hepatitis: a prospective observation of 2215 patients. J Hepatol. 1998;28:930–8.
2. Hoofnagle JH, di Bisceglie AM. The treatment of chronic viral hepatitis. N Engl J Med. 1997;336:347–56.
3. Ghany MG, Strader DB, Thomas DL, Seeff LB. Diagnosis, management, and treatment of hepatitis C: an update. Hepatology. 2009;49:1335–74.
4. Shiffman ML, Hofmann CM, Contos MJ, Luketic VA, Sanyal AJ, Sterling RK, et al. A randomized, controlled trial of maintenance inteferon therapy for patients with chronic hepatitis C virus and persistent viremia. Gastroenterology. 1999;117:1164–72.
5. Nomura H, Kashiwagi Y, Hirano R, Tanimoto H, Tsutsumi N, Higashi M, et al. Efficacy of low dose long-term interferon monotherapy in aged patients with chronic hepatitis C genotype 1 and its relation to alpha-fetoprotein: a pilot study. Hepatol Res. 2007;37:490–7.
6. Akuta N, Suzuki F, Kawamura Y, Yatsuji H, Sezaki H, Suzuki Y, et al. Efficacy of low-dose intermittent interferon-alpha monotherapy in patients infected with hepatitis C virus genotype 1b who were predicted or failed to respond to pegylated interferon plus ribavirin combination therapy. J Med Virol. 2008;80:1363–9.
7. Di Bisceglie AM, Shiffman ML, Everson GT, Lindsay KL, Everhart JE, Wright EC, et al. Prolonged therapy of advanced chronic hepatitis C with low-dose peginterferon. New Engl J Med. 2008;359:2429–41.
8. Sugahara K, Togashi H, Takahashi K, Onodera Y, Sanjo M, Misawa K, et al. Separate analysis of asialoglycoprotein receptors in the right and left hepatic lobes using Tc-99m-GSA SPECT. Hepatology. 2003;38:1401–9.
9. Tanabe J, Izawa A, Takemi N, Miyauchi Y, Torii Y, Tsuchiyama H, et al. Interferon-beta reduces the mouse liver fibrosis induced by repeated administration of concanavalin A via the direct and indirect effects. Immunology. 2007;122:562–70.
10. Kumada H, Okanoue T, Onji M, Moriwaki H, Izumi N, Tanaka E, et al. Guidelines for the treatment of chronic hepatitis and cirrhosis due to hepatitis C virus infection for the fiscal year 2008 in Japan. Hepatol Res. 2010;40:8–13.
11. Yagura M, Murai S, Kojima H, Tokita H, Kamitsukasa H, Harada H. Changes of liver fibrosis in chronic hepatitis C patients with no response to interferon-alpha therapy: including quantitative assessment by a morphometric method. J Gastroenterol. 2000;35:105–11.
12. Murata M, Nabeshima S, Kikuchi K, Yamaji K, Furusyo N, Hayashi J. A comparison of the antitumor effects of interferon-alpha and beta on human hepatocellular carcinoma cell lines. Cytokine. 2006;33:121–8.
13. Izuma M, Kobayashi K, Shiina M, Ueno Y, Ishii M, Shimosegawa T, et al. In vitro cytokine production of peripheral blood mononuclear cells in response to HCV core antigen stimulation during interferon-beta treatment and its relevance to sCD8 and sCD30. Hepatol Res. 2000;18:218–29.
14. Nelson DR, Tu Z, Soldevila-Pico C, Abdelmalek M, Zhu H, Xu Y, et al. Long-term interleukin 10 therapy in chronic hepatitis C patients has a proviral and anti-inflammatory effect. Hepatology. 2003;38:859–68.

Oncogene (2009) 28, 469–478

www.nature.com/onc

ORIGINAL ARTICLE

A novel mouse model of hepatocarcinogenesis triggered by AID causing deleterious p53 mutations

A Takai[1], T Toyoshima[3], M Uemura[3], Y Kitawaki[2], H Marusawa[1], H Hiai[3], S Yamada[4], IM Okazaki[2], T Honjo[2], T Chiba[1] and K Kinoshita[3]

[1]*Department of Gastroenterology and Hepatology, Graduate School of Medicine, Kyoto University, Kyoto, Japan;* [2]*Department of Immunology and Genomic Medicine, Graduate School of Medicine, Kyoto University, Kyoto, Japan;* [3]*Shiga Medical Center Research Institute, Moriyama, Japan and* [4]*Mikasa Laboratory, Immuno-Biological Laboratories Co., Ltd, Mikasa, Japan*

Activation-induced cytidine deaminase (AID), the only enzyme that is known to be able to induce mutations in the human genome, is required for somatic hypermutation and class-switch recombination in B lymphocytes. Recently, we showed that AID is implicated in the pathogenesis of human cancers including hepatitis C virus (HCV)-induced human hepatocellular carcinoma (HCC). In this study, we established a new AID transgenic mouse model (TNAP-AID) in which AID is expressed in cells producing tissue-nonspecific alkaline phosphatase (TNAP), which is a marker of primordial germ cells and immature stem cells, including ES cells. High expression of TNAP was found in the liver of the embryos and adults of TNAP-AID mice. HCC developed in 27% of these mice at the age of approximately 90 weeks. The HCC that developed in TNAP-AID mice expressed α-fetoprotein and had deleterious mutations in the tumour suppressor gene *Trp53*, some of which corresponded to those found in human cancer. In conclusion, TNAP-AID is a mouse model that spontaneously develops HCC, sharing genetic and phenotypic features with human HCC, which develops in the inflamed liver as a result of the accumulation of genetic changes.
Oncogene (2009) **28,** 469–478; doi:10.1038/onc.2008.415; published online 10 November 2008

Keywords: hepatic cancer; stem cell marker; activation-induced cytidine deaminase; Cre recombinase; somatic mutation; animal model

Introduction

It is widely recognized that mutations of oncogenes, tumour suppressor genes and genomic stability genes play pivotal roles in cancer development (Vogelstein and Kinzler, 2004). Despite remarkable progress in our knowledge of the molecular mechanisms of individual cancer-related genes, surprisingly little is known about the fundamental aspects of when and how mutations are introduced into what kind of cell populations (for example, differentiated cells versus tissue stem cells).

To address this problem, a new mechanism of mutagenesis for cancer development has recently been proposed (Kinoshita and Nonaka, 2006; Marusawa, 2008). It hypothesizes that at least some cancer-related mutations are introduced by activation-induced cytidine deaminase (AID), an enzyme that is expressed in activated B lymphocytes, and is required for somatic hypermutation (SHM) and class-switch recombination of antibody genes (Honjo *et al.*, 2002). The hypothesis is based on the following observations: (1) AID can induce mutations in non-B cells (Yoshikawa *et al.*, 2002); (2) AID transgenic mice develop various tumours, including T-cell lymphoma and lung microadenoma (Okazaki *et al.*, 2003) and (3) AID can be induced in human hepatic, gastric and biliary epithelial cells when stimulated with pro-inflammatory cytokines, such as transforming growth factor-β and tumor necrosis factor-α, and when challenged with pathogens, such as hepatitis C virus (HCV) and *Helicobacter pylori*. AID is detected in the liver, stomach and bile duct in humans (Kou *et al.*, 2006; Endo *et al.*, 2007; Matsumoto *et al.*, 2007; Komori *et al.*, 2008). On the basis of this evidence, AID is a potential candidate for a mutagen in human cancers.

To substantiate this hypothesis, there is an urgent need for the establishment of an AID transgenic mouse model that recapitulates the development of human cancer. However, we have found earlier that it is difficult to analyse epithelial tumours of tissues other than lymphoid malignancies in a transgenic mouse model with constitutive and ubiquitous AID expression because of early death of the mice from lethal T-cell lymphoma (Okazaki *et al.*, 2003).

We generated earlier AID transgenic mice that can express AID conditionally in a Cre-recombianase-dependent manner (AID conditional transgenic, AID cTg) and reported B-cell-specific AID transgenic mice

Correspondence: Dr K Kinoshita, Evolutionary Medicine, Shiga Medical Center Research Institute, 5/4/1930, Moriyama, Shiga 524-8524, Japan.
E-mail: kkinoshi.shigamed@mac.com
Received 30 June 2008; revised 30 September 2008; accepted 14 October 2008; published online 10 November 2008

obtained by crossing AID cTg mice with B-cell-specific Cre transgenic mice (Muto *et al.*, 2006). In this study, we used a different Cre transgenic mouse line that expresses Cre in cells producing tissue nonspecific alkaline phosphatase (TNAP), as the mating partner of AID cTg mice.

TNAP is a member of the alkaline phosphatase family encoded by the *Akp2* gene and alternatively designated alkaline phosphatase 2, liver. As TNAP is also known as a marker of primordial germ cells and immature stem cells, including ES cells (Urven *et al.*, 1993; Kues *et al.*, 2005; Wang *et al.*, 2005), we initially speculated that AID expression in TNAP-positive cells might contribute to the development of tumours of germ cell origin. However, the resulting mice frequently developed hepatocellular carcinoma (HCC) but not germ cell tumours or lethal lymphomas. Histological and molecular analyses of HCC revealed genetic and phenotypic similarities to human tumours, including deleterious mutations in the p53 gene and the expression of α-fetoprotein, a well-known marker of human HCC. This mouse model should be useful for studies on the prevention and treatment of hepatic cancer, which is a major health concern worldwide.

Results

We crossed AID cTg mice with TNAP-Cre mice (Lomeli *et al.*, 2000; Figures 1a and b). AID cTg mice possess a CAG promoter-driven AID transgene, whose expression is blocked by insertion of the gene encoding enhanced green fluorescent protein (hereafter GFP) flanked by two loxP sites (Figure 1a). Therefore, the expression of Cre recombinase removes GFP and induces AID expression (Muto *et al.*, 2006). TNAP-Cre mice were generated by inserting the coding sequence of Cre recombinase into the *Akp2* locus of the 129/Sv mouse genome, and Cre was expressed in primordial germ cells in the embryonic genital ridge region (Lomeli *et al.*, 2000). We crossed homozygous female AID cTg mice on a C57BL/6 background with heterozygous male TNAP-Cre mice to obtain double-transgenic mice (TNAP-AID) and their littermate control AID cTg mice. Non-transgenic (wild-type, WT) and TNAP-Cre control mice on a C57BL/6:129/Sv hybrid background were obtained by mating female C57BL/6 mice with heterozygous male TNAP-Cre mice (Figure 1b). Accordingly, a total of 101 mice were prepared, which included 28 TNAP-AID, 29 AID cTg, 16 TNAP and 28 WT mice.

Most mice were viable at 90 weeks (Figure 1c), whereas in our earlier study, most AID transgenic mice died because of the lethal lymphoid malignancies, majority of which died within 50 weeks (Okazaki *et al.*, 2003). Although TNAP is expressed in primordial germ cells, we did not observe any incidence of testicular or ovarian tumours in TNAP-AID mice. Instead of germ cell tumours, we frequently observed macroscopic liver tumours in TNAP-AID mice. Table 1 summarizes

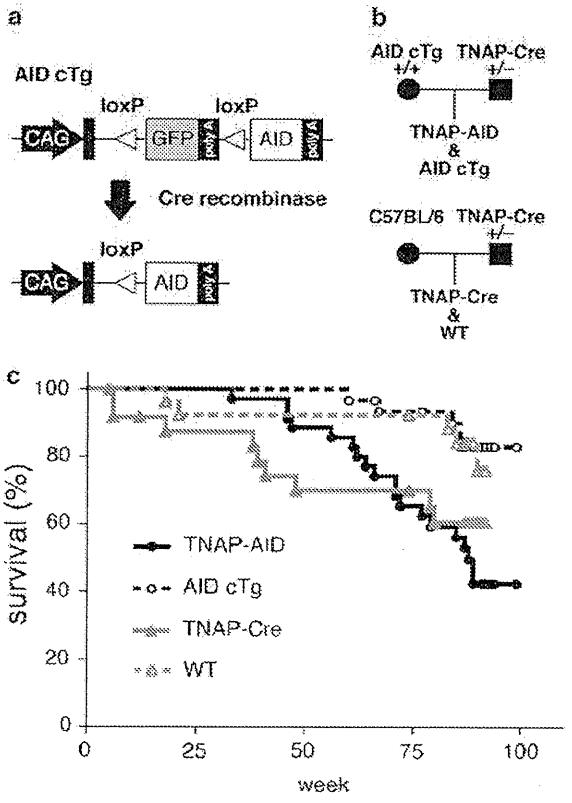

Figure 1 Generation of TNAP-AID mice and their controls. (**a**) Structure of transgene used to generate AID conditional transgenic mice (AID cTg) and the structure after Cre-mediated recombination. Arrows indicate the CAG promoter and rectangles indicate exons. Grey and open boxes represent the coding sequences of GFP and AID, respectively. A polyadenylation signal (poly A) is attached after each coding sequence. Triangles indicate loxP sites. (**b**) Mating scheme. For genotype abbreviations, see text. (**c**) Kaplan–Meier survival curves for the four genotype groups.

the frequency and spectrum of tumours that developed in TNAP-AID and control mice. Interestingly, liver tumours were observed in TNAP-AID mice but not in the control groups; the difference between TNAP-AID and AID cTg mice ($P=0.017$) and that between TNAP-AID and WT mice ($P=0.018$) was significant. There were no differences among the groups with regard to weights of body, liver, spleen and kidneys in healthy mice (data not shown).

Macroscopically, multiple liver nodules were frequently observed in mice with liver tumour (4 out of 15; Table 1, Figure 2a). The number and size of the nodules varied. Microscopically, liver tumours showed various degrees of cellular atypia, from adenoma to HCC with occasional 'carcinoma in adenoma', suggesting ongoing progression. The expression of α-fetoprotein, a marker of human HCC, was detected in the tumours by immunohistochemical analyses (Figure 2b) and quantitative reverse transcription PCR (qRT-PCR) (Supplementary Figure 1). None of the tumours showed

Table 1 Frequencies of tumours observed in TNAP-AID and control mice

Genotype	*Mean age at killing (weeks)*	*HCC*	*Lymphoma*	*Lung cancer*	*Stomach cancer*
TNAP-AID (15)	88.5	26.7% (4)	40.0% (6)	6.7% (1)	6.7% (1)
AID-cTg (24)	89.9	0.0% (0)	29.2% (7)	0.0% (0)	0.0% (0)
TNAP-Cre (14)	88.4	0.0% (0)	0.0% (0)	0.0% (0)	0.0% (0)
WT (23)	89.1	0.0% (0)	17.4% (4)	0.0% (0)	0.0% (0)

Abbreviations: HCC, hepatocellular carcinoma; WT, wild type.
Frequencies were calculated from the numbers of mice with macroscopic tumours of the indicated organs at approximately 90 weeks of age. Numbers in parentheses are the number of individuals killed for tumour inspection (genotype column) and those with macroscopic tumours (right four columns).

nuclear localization of β-catenin protein (data not shown).

Sequences of some tumour suppressor genes and oncogenes in the tumours were determined. Significant numbers of mutations were observed in the *Trp53* gene encoding the p53 protein (Table 2). The non-transcribed region upstream of the promoter did not contain mutations, an observation that is consistent with the transcription dependence of mutagenesis by AID (Yoshikawa *et al.*, 2002). Majority of mutations were single-base substitutions with significant GC bias, another footprint of AID (Figure 3a) (Yoshikawa *et al.*, 2002). There was no significant correlation between the distribution of mutations and those of SHM hot spot motifs (RGYW/WRCY) and DNA secondary structures (Supplementary Figure 2). Interestingly, the mutation frequency was the highest in cancer tissues followed by non-cancerous TNAP-AID liver and lowest in normal liver of WT mice, which corresponds to the PCR error rate or the background rate in this assay. The increase in mutation frequency in HCC compared with non-cancerous liver was because of the increase in single-base insertion events mostly at the homonucleotide tracts, leading to frameshift mutations in the 5′-half of the coding region (Table 2 and Figure 3b). Most of TNAP-AID liver mutations occurred in the DNA-binding domain of p53, which is critical for its function (Table 3).

Although small volumes (approximately 50 mm^3) of normal and cancerous liver tissues were dissected for mutation analysis, the identified mutations were quite diverse, suggesting that the sampled tissue block contained multiple HCC nodules, each representing monoclonal expansion. Such heterogeneity was verified by two independent series of PCR, plasmid cloning and sequencing for the same sample: there were few overlaps of mutations. For example, 8 and 7 clones derived from HCC of mouse TA113 contained nonsynonymous point mutations out of sequenced 27 and 40 clones in the first and second experiment, respectively. The mutation patterns were completely different except C808G (R270G), which appeared thrice and once in the first and the second trial, respectively. Table 3 lists the combined results of the two experiments. The most frequent mutations were C790T(R264W) and C808G(R270G), the latter corresponding to one of the second most important mutational targets (R273) in human cancers (Figure 3b, top). Despite extensive sequencing, no mutations were found in *Myc*, *Pten* and *Cdkn2a* (p16 and $p19^{Arf}$) genes (Supplementary Figure 3). The *Trp53* mutation frequency in the thymus was significantly lower than in the liver of TNAP-AID mice, which is consistent with the lack of lethal T-cell lymphomagenesis (Table 2).

To determine why liver tumours developed, TNAP expression in various organs was examined by qRT-PCR in E14.5 embryos and 53- to 74-week-old adult mice of strain C57BL/6. TNAP was ubiquitously expressed at a relatively high level in the liver and intestine of the embryos and in the liver and testis of the adults (Figure 4a). In agreement with this wide distribution of TNAP expression, GFP expression in TNAP-AID mice was absent in most organs in adults (Figure 4c). The substantial levels of AID expression were confirmed by qRT-PCR (Figure 4b) and western blotting (Figure 4d) in various organs of the adult TNAP-AID mice but not of AID cTg mice. The presence of AID protein and loss of GFP were detected in the non-cancerous liver sections of TNAP-AID mice (Figure 5). Taken together, these findings suggest that constitutive AID expression in hepatic lineage, including fetal and adult liver, contributes to the high incidence of liver tumours.

As reported for AID transgenic mice with the ubiquitous promoter, lymphomas were observed in TNAP-AID mice (Table 1). Although the frequency of lymphomas in the TNAP-AID group was higher than those in the other groups, the differences between TNAP-AID and AID cTg mice ($P=0.508$) and those between TNAP-AID and WT mice ($P=0.150$) were not statistically significant. The survival curve analysis (Figure 1c) suggested that there was no significant difference between the TNAP-AID and TNAP-Cre groups ($P=0.515$), indicating that the lymphomas in TNAP-AID mice were less aggressive than those in the transgenic mice with ubiquitous AID expression. Histologically, the lymphomas in TNAP-AID mice exhibited nodular appearance, which was different from that of the diffusely infiltrating lymphoma that develops in the ubiquitous promoter-driven AID transgenic mice (data not shown). This difference suggests that different mechanisms underlie tumorigenesis of lymphoid cells between these mice. We confirmed that GFP expression and Cre-mediated excision of GFP occurred efficiently in CD3-positive T cells of AID cTg and TNAP-AID mice, respectively (Supplementary Figure 4). This suggests that AID is expressed in T cells of TNAP-AID mice.

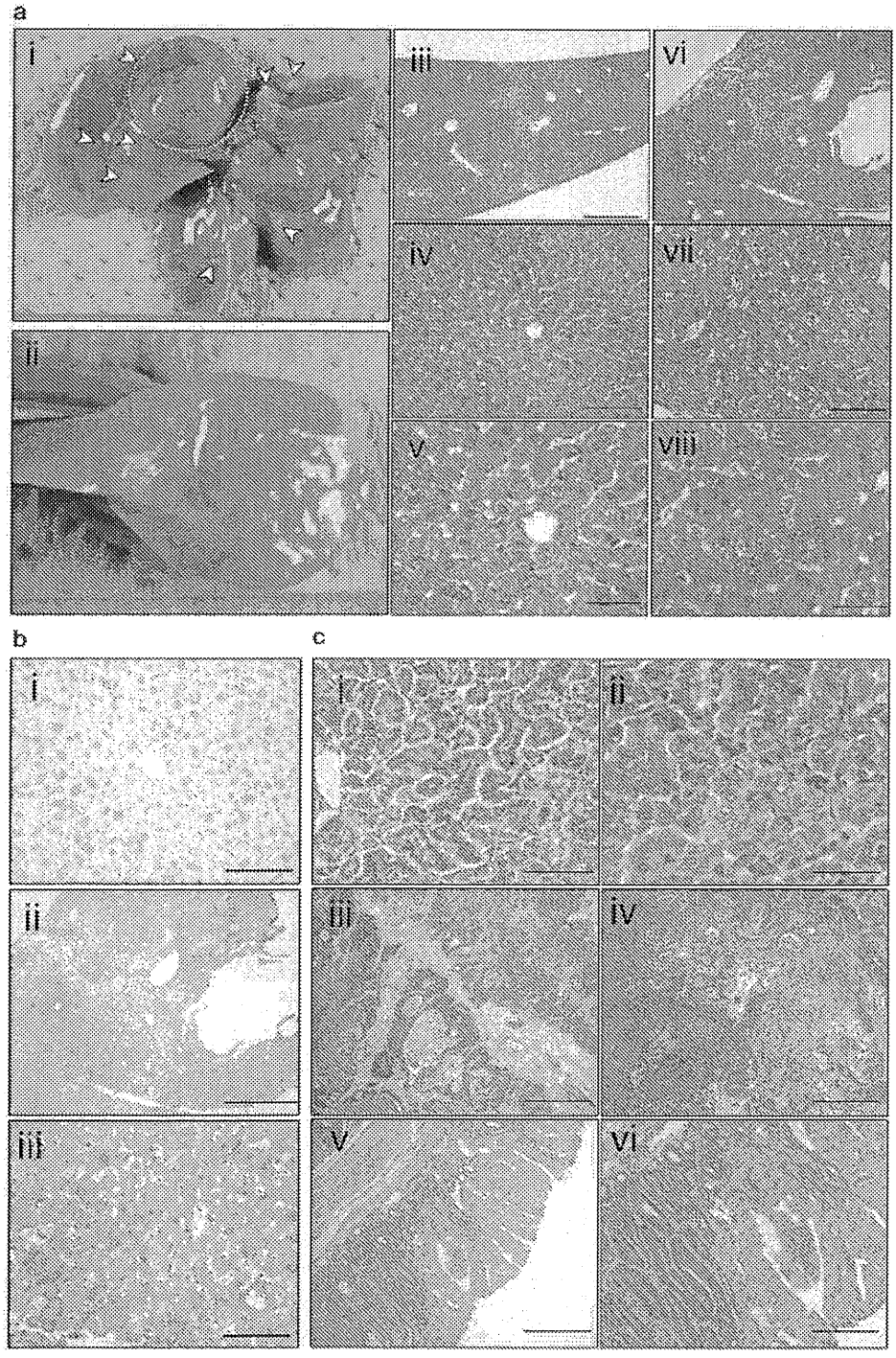

Figure 2 Tumours developed in TNAP-AID mice. (**a**) Macroscopic (i and ii) and microscopic (haematoxylin and eosin (HE) stain) images of HCC (i, ii, vi, vii and viii) that developed in a TNAP-AID mouse and non-cancerous liver of the same animal (iii, iv and v). In panel ai, arrowheads indicate liver tumour nodules. The largest nodule is encircled with a dotted line, and its cut surface is shown in panel aii). Scale bars are 1 mm (iii and iv), 500 μm (iv and vii) and 200 μm (v and viii). (**b**) Immunohistochemistry for α-fetoprotein of the normal liver (i) and HCC (ii and iii), which are serial sections of images shown in panel aiv, avi and aviii, respectively. Scale bars are 500 μm (i and iii) and 1 mm (ii). (**c**) Microscopic images (HE stain) of cancer of the lung (i and ii) and the stomach (iii and iv, squamous cell carcinoma; v and vi, adenocarcinoma). Scale bars are 200 μm (i, iv and vi), 100 μm (ii) and 500 μm (iii and v).

Table 2 *Trp53* gene mutation profiles in liver and HCC of TNAP-AID mice

Target	*Genotype*	*WT*	*TNAP-AID*	*HCC*	*Gastric cancer*	*Thymus*
	Tissue	*Normal liver*	*Non-cancerous liver*			
Transcribed region	Mutated/total clones	4/48	11/49	33/112	7/34	0/21
	Mutated (pm:ins:del)/total bases	4 (2:1:1)/52 487	12 (10:2:0)/55 321	42 (27:13:2)/127 674	9 (5:3:1)/38 789	0/24 446
	Mutation frequency × 10^4	0.76	2.17	3.29	2.32	0.00
Non-transcribed region	Mutated/total clones	0/16	0/15	0/16		
	Mutated (pm:ins:del)/total bases	0/13 828	0/12 613	0/13 947		
	Mutation frequency × 10^4	0.00	0.00	0.00		

Abbreviations: HCC, hepatocellular carcinoma; WT, wild type.
Mutation frequency of the transcribed and non-transcribed regions of the *Trp53* gene of the normal liver from two WT mice (87- and 89-week-old) and non-cancerous liver, HCC and thymic tissues from three TNAP-AID mice (92- to 94-week-old). Mutated base numbers are shown with numbers of point mutations (pm), insertions (ins) and deletions (del) in parentheses.

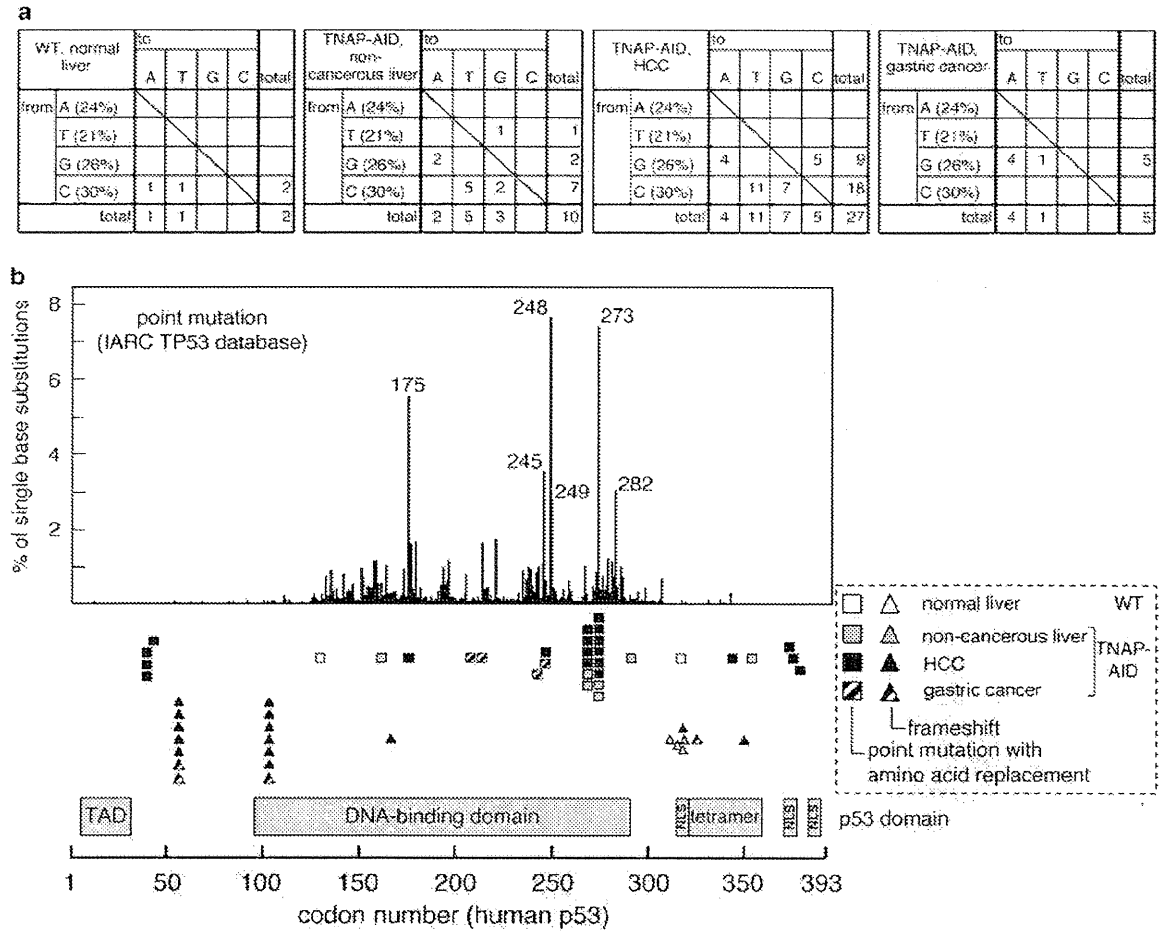

Figure 3 *Trp53* gene mutation profiles in liver and HCC of TNAP-AID mice. (**a**) Base substitution patterns seen in liver of WT mice (left), non-cancerous liver of TNAP-AID mice (centre) and HCC of TNAP-AID mice (right) extracted from the same data sets as those used for the mutation frequency analysis in Table 2. Percentages in parentheses are compositions of the indicated bases in the sequenced region. (**b**) Top: Distribution of *TP53* somatic mutations in human cancer, reproduced from the IARC TP53 Database (version R12), November 2007 (http://www-p53.iarc.fr/) (Petitjean *et al.*, 2007). Middle: Distribution of mouse *Trp53* mutations found in WT and TNAP-AID mouse liver. Codon positions are converted into human equivalents. Squares and triangles indicate point mutations with amino acid replacements and frameshifts, respectively. Open, grey, filled and hatched symbols indicate normal liver of WT mice, non-cancerous liver, HCC and gastric cancer of TNAP-AID mice, respectively. Bottom: p53 domain structure with transactivation (TAD), DNA-binding and tetramerization domains and nuclear localization signal (NLS).

Table 3 Predicted amino acid replacements observed in three TNAP-AID mice (TA113, TA114 and TA128), corresponding human mutations and affected domains of p53

Tissue	*Mutation*		*Mouse ID*	*Mutated/total clone*	*Human-equivalent codon*	*Domain*	*Functional assays*[a]		*Count*[a]
	Nucleotide	*Codon*					*Transactivation class*	*Structure-based prediction*	
TNAP-AID, non-cancerous liver	G472A	A158T	TA113	1/26	A161T	DNA binding	Partially functional	Non-functional	73
	C790T	R264W	TA128	2/23	R267W	DNA binding	Non-functional	Non-functional	25
	C808G	R270G	TA128	2/23	R273G	DNA binding	Non-functional	Non-functional	14
	G860A	R287H	TA113	1/26	R290H	DNA binding	Supertrans	NA	29
	C1049T	A350V	TA113	1/26	A353V	Tetramerization	Supertrans	NA	0
TNAP-AID, HCC	G119C	C40S	TA113	2/67	None	Transactivation	NA	NA	NA
			TA114	1/33					
	G127A	D43N	TA113	1/67	D42N	Transactivation	Functional	NA	0
	C532T	R178C	TA114	1/33	R175C	DNA binding	Partially functional	Non-functional	24
	G729A	M243I	TA113	1/67	M246I	DNA binding	Non-functional	Functional	32
	C790T	R264W	TA113	3/67	R267W	DNA binding	Non-functional	Non-functional	25
			TA114	1/33					
	C808G	R270G	TA113	4/67	R273G	DNA binding	Non-functional	Non-functional	14
			TA114	2/33					
	G1020C	E340D	TA113	1/67	E343D	Tetramerization	Functional	NA	0
	G1112A	G371D	TA113	1/67	G374D	Regulation/NLS	Functional	NA	0
	C1118G	S373C	TA113	1/67	S376C	Regulation/NLS	Functional	NA	0
	G1127C	R376P	TA113	1/67	R379P	Regulation	Partially functional	NA	0
TNAP-AID, gastric cancer	G613T	D205Y	TA114	1/34	D208Y	DNA binding	Non-functional	Functional	1
	G629A	R210H	TA114	1/34	R213Q	DNA binding	Non-functional	Non-functional	34
	G716A	C239Y	TA114	1/34	C242Y	DNA binding	Non-functional	Non-functional	51
	G729A	M243I	TA114	1/34	M246I	DNA binding	Non-functional	Functional	32

Abbreviation: NA, data not available.
For details, visit the IARC website.
[a]Based on the data presented in the IARC website and described in the legend of Figure 3. Functional assays are predicted as impacts of mutations in yeast assays and structural computation. Count is the number of the entries in the database.

Macroscopic tumours of other organs included one case of lung adenocarcinoma and one case of gastric cancer (squamous cell carcinoma) (Table 1 and Figure 2c). These rare tumours were restricted to the TNAP-AID group and likely to be caused by AID expression. However, the small number of tumours precludes a quantitative discussion on causal relationships, except for liver tumours. Sequencing analysis revealed that *Trp53* mutation frequency in gastric cancer tissue was $2.32/10^4$, a comparable level to that observed in HCC tissues (Tables 2 and 3 as well as Figure 3). Unfortunately, we could not carry out mutation analyses on the lung cancer tissue because of its small size. We did not examine microscopic tumours except for subpleural lung microadenomas, which were observed in the TNAP-AID mice, a finding similar to that in the AID transgenic mice in our earlier study (Okazaki *et al.*, 2003). In addition, two cases of gastric adenocarcinoma were found incidentally by microscopic examination (Figure 2c), suggesting that many microscopic tumours may have been overlooked.

Discussion

Here we describe TNAP-AID mice as a novel model of hepatocarcinogenesis, which occurs as a result of the accumulation of mutations in chronically inflamed liver in humans, often caused by infection with hepatitis viruses. The TNAP-AID mouse model exhibits several characteristics of human HCC, in that the mice develop HCC spontaneously and the HCC tissue expresses α-fetoprotein and that it has the p53 gene mutations, some of which cause the same amino acid replacements as those seen in human tumours. Earlier HCC mouse models include mice with genetic modifications of *Lkb1*, *Mdr2*, *Aox* and *Pten* genes (Fan *et al.*, 1998; Nakau *et al.*, 2002; Horie *et al.*, 2004; Katzenellenbogen *et al.*, 2006), transgenic mice overexpressing c-myc, transforming growth factor-α, transforming growth factor-β1, HBx of hepatitis B virus and HCV core (Sandgren *et al.*, 1989; Kim *et al.*, 1991; Murakami *et al.*, 1993; Koike *et al.*, 1994, 2002; Factor *et al.*, 1997; Riehle *et al.*, 2008) and chemical- or diet-induced HCC (Sell, 2001; Maeda *et al.*, 2005; Ma *et al.*, 2006; Sakurai *et al.*, 2006). In contrast to these models, our TNAP-AID model is unique because it does not arbitrarily target specific oncogenes, tumour suppressors or stability genes. In addition, it does not use chemical mutagens or specific dietary conditions that are not associated with human HCC. The development of *Trp53* mutations is another feature of this model because it is unprecedented in any earlier mouse HCC models as mentioned above.

Liver tumours were occasionally observed in our earlier AID transgenic mice (Endo *et al.*, 2007). However, it was difficult to use these mice as a liver tumour model because of early death from lethal lymphomas. Trials to detect *Trp53* mutations in the liver tumour failed (data not shown). Even the T-cell

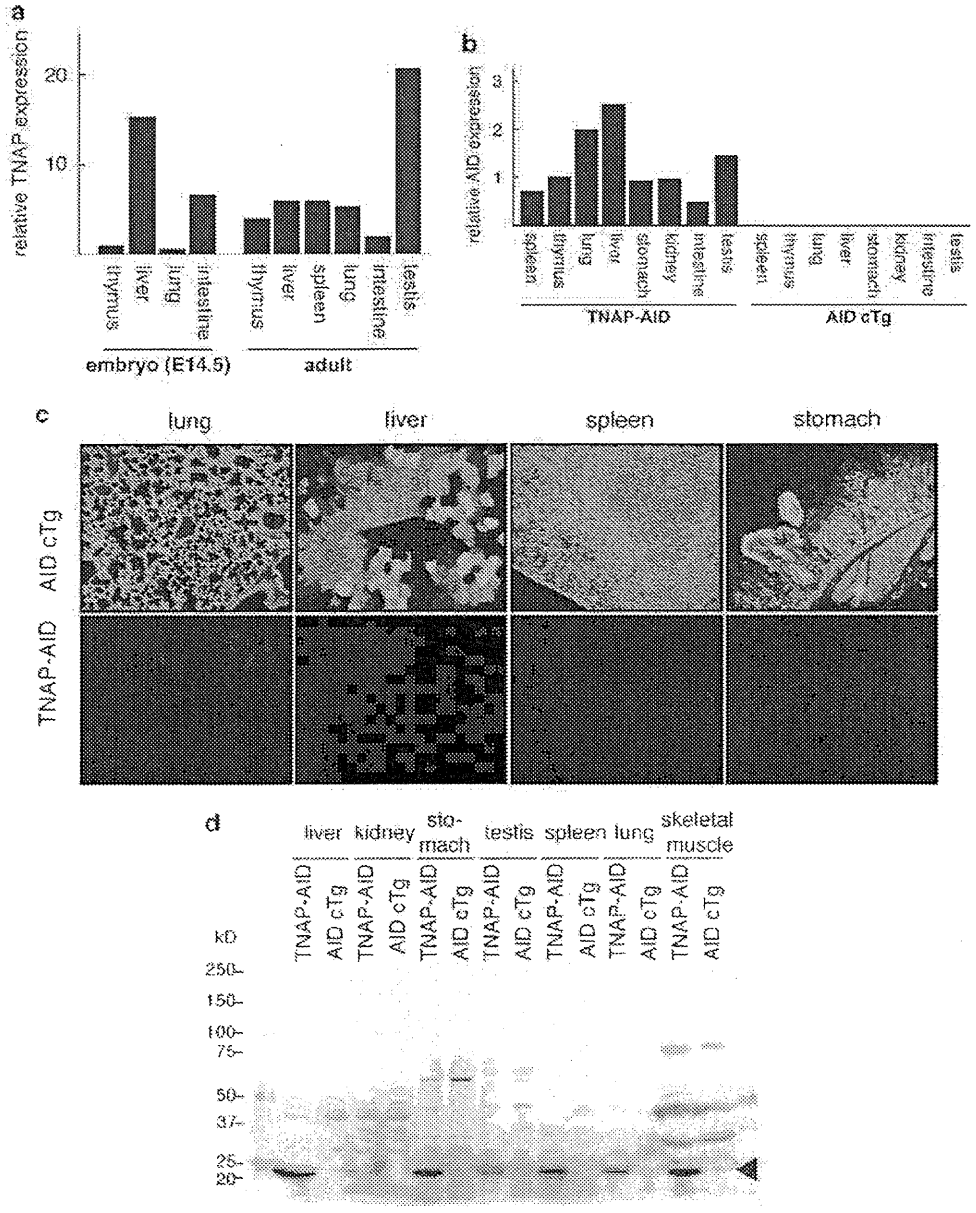

Figure 4 Expression analysis of TNAP-AID mice. (**a**) Results of qRT-PCR for TNAP gene (*Akp2*) calibrated by the amount of ribosomal 18S RNA for indicated organs of adult mice (53- and 74-week-old) and four E14.5 embryos. The graph shows average results for the indicated groups. (**b**) Results of qRT-PCR for transgene-derived AID expression. (**c**) GFP fluorescence in frozen sections of GFP from the indicated organs and animals. A mosaic pattern of GFP expression in the liver of AID cTg mice was always observed, which may be attributed to the integration site of the transgene. (**d**) Western blot analysis using anti-AID monoclonal antibody MAID-1 for the lysates of indicated organs of 42-week-old TNAP-AID and AID cTg mice. Arrowhead indicates the position of the AID band. Comparable intensities of nonspecific bands indicate equal loading of extracts between TNAP-AID and AID cTg lanes.

lymphomas that developed in the earlier AID transgenic mice did not harbour *Trp53* mutations (Kotani *et al.*, 2005). Therefore, the TNAP-AID mouse model is the first model in which *Trp53* mutations can be detected unequivocally in non-cancerous tissues as well as in cancerous tissues that express AID. In spite of these differences, the two independent AID transgenic mice lines commonly developed liver tumours, making it unlikely that liver tumours in TNAP-AID mice are ascribed to unexpected variables such as the transgene integration sites and the segregation of relevant loci upon crossing of mice with different genetic backgrounds. However, the possibility that these variables somewhat modified the tumour frequency cannot be excluded.

The overlap of mutational hot spots between TNAP-AID and human HCC (Table 3 and Figure 3b) suggests that these mutations induced by AID have critical roles.

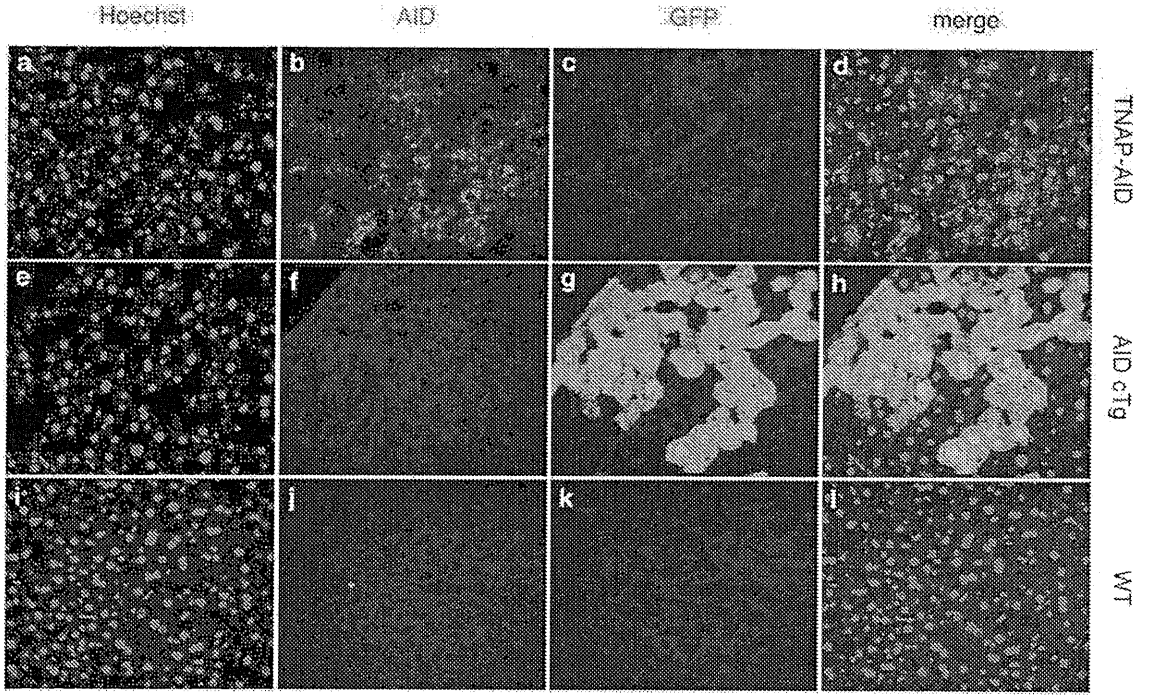

Figure 5 Immunohistochemical analysis of frozen liver sections from TNAP-AID (**a–d**), AID cTg (**e–h**) and WT (**i–l**) mice. (**a**, **e** and **i**) Hoechst 33342 staining; (**b**, **f** and **j**) AID immunostaining; (**c**, **g** and **k**) GFP fluorescence; (**d**, **h** and **l**) merge of the three colours.

The lack of *Trp53* mutations in the earlier transgenic mouse model may reflect a different evolutionary path from the initiation to progression of liver tumours between the two models despite the common involvement of AID. This difference may be related to the difference in the frequency and aggressiveness of lymphomas between TNAP-AID and the earlier AID transgenic mouse, as discussed below. The point mutations observed in *Trp53* are likely to be a direct effect of AID activity, because they share some molecular footprints with SHM of the immunoglobulin genes, including GC bias, frequent C-to-T transitions and transcription dependence. However, there was no correlation between the distributions of mutations and SHM hot spot motifs or DNA secondary structures in the *Trp53* sequence. As these parameters show only weak association even for SHM, the small numbers of point mutations observed in this study may not be sufficient to achieve statistical significance. On the other hand, single-base insertions causing frameshifts in *Trp53* were frequently observed in HCC but not in the non-cancerous liver of TNAP-AID mice. As single-base insertions are relatively rare in SHM induced by AID, these might be caused by genetic instability (for example, impaired mismatch repair) acquired during the progression of the tumours.

The presence of mutations in non-cancerous tissue expressing AID is reminiscent of a study on human patients with chronic hepatitis (Kou *et al.*, 2006), together suggesting a causal role of AID in tumorigenesis. It is noteworthy that the mutations corresponding to two mutational hot spots in *TP53* gene encoding human p53 (R273 and R175) were included in mutations found in TNAP-AID HCC. Other mutations were mapped close to the human hot spots (M246 and R267) (Figure 3b and Table 3). Among them three patterns of amino acid replacement, C40S, R264W and R270G, were observed repeatedly in multiple individuals. Such repeated appearance of the specific mutations in different individuals may indicate their significance in tumorigenesis. In addition to these common mutations, HCC and the non-cancerous liver contained quite diverse mutation patterns, which parallels heterogeneity of *TP53* mutations within human HCC occurred in a single individual and is consistent with the 'field cancerization' model (Thorgeirsson and Grisham, 2002).

The utility of the TNAP-AID mouse as a human HCC model depends partly on the lack of lethal lymphomas that were observed in almost all AID transgenic mice in our earlier study. To examine the reason why lymphomas were infrequent and less aggressive in the TNAP-AID model, mutations caused by AID and its expression in T lymphocytes of TNAP-AID mice were analysed by sequencing the *Trp53* coding sequence (Table 2) and flow cytometry (Supplementary Figure 4). From these analyses, it was found that *Trp53* was not mutated, but AID was expressed in the thymocytes of the TNAP-AID mice. The level of AID expression in the thymus of TNAP-AID mice was half than that seen in the earlier AID transgenic line in a qRT-PCR analysis (data not shown). We speculate that the difference in the levels of AID expression in T cells

may be one of the reasons for this, although the difference in the genetic background (C57BL/6:129/Sv hybrid versus pure C57BL/6) cannot be excluded.

The TNAP-AID mice did not develop germ cell tumours despite the expression of AID in the testes (Figure 4d) and the absence of GFP in the seminiferous tubules and oocytes of the ovaries (data not shown). We reported earlier the lack of lymphomagenesis in B-cell-specific AID transgenic mice obtained by crossing the same AID cTg line with CD19-Cre mice (Muto *et al.*, 2006), suggesting that some protective mechanism might exist in B cells, which have physiological expression of AID. A similar reason might apply to germ cells because AID has been reported to be expressed physiologically in the human testis (Schreck *et al.*, 2006) and mouse ovary (Morgan *et al.*, 2004).

To conclude, we generated a new line of AID transgenic mice that develop HCC but not lethal T-cell lymphoma. We consider that the TNAP-AID mouse model is useful for human HCC studies because it has been shown that AID is induced in the human pre-cancerous conditions of chronic hepatitis and cirrhosis (Kou *et al.*, 2006). The relatively long latency before HCC development in this model is reasonable, considering that it is a physiological recapitulation of a human tumour phenotype that takes decades to develop.

Materials and methods

Mice

The AID cTg mice (line 20) on a C57BL/6 background (Muto *et al.*, 2006) were self-crossed to obtain homozygous transgenic mice, which were maintained in a specific pathogen-free facility at the Kyoto University Faculty of Medicine and Shiga Medical Center. This mouse line has been deposited at the Riken Bioresource Center (Tsukuba, Japan; No. RBRC00892). The TNAP-Cre mice (Lomeli *et al.*, 2000) were gifted by Dr Andras Nagy (Mount Sinai Hospital, Toronto, Canada) and maintained by self-crossing between the heterozygous mice. C57BL/6 mice were purchased from Shimizu Laboratory Supplies Co., Ltd (Kyoto, Japan). All mice were fed *ad libitum* and were killed by cervical dislocation for censoring, or observed until spontaneous death. Upon censoring and spontaneous death, the numbers of macroscopic tumours were counted after laparotomy and thoracotomy. Kaplan–Meier survival curves were analysed using Prism 4.0 software (Graphpad, San Diego, CA, USA). All animal experiments were approved by the Ethical Committee for Animal Experiments and performed under the Guidelines for Animal Experiments of Kyoto University and Shiga Medical Center.

Histology and immunohistochemistry

Paraffin-embedded mouse organs were sectioned and stained with haematoxylin and eosin. α-Fetoprotein was detected using anti-α-fetoprotein antibody (Dako, Glostrup, Denmark) and an ABC kit (Vector, Burlingame, CA, USA) for paraffin-embedded sections of formalin-fixed liver. For AID immunostaining, freshly isolated liver was fixed in 4% paraformaldehyde in phosphate-buffered saline on ice for 2 h and immersed in 30% sucrose for 18 h. After embedding in OCT compound (Sakura Fineteck Japan, Tokyo, Japan) in liquid nitrogen, 8-μm sections were sliced and mounted on glass slides. Hoechst 33342 dye was used to visualize nuclei. AID protein was detected using the monoclonal anti-AID antibody, MAID-2 (Tsuji *et al.*, 2008), with peroxidase-labelled donkey F(ab')2 anti-rat IgG (Jackson ImmunoResearch, West Grove, PA, USA) and signal amplification using TSA Plus DNP and TSA Plus TMR kits (Perkin Elmer, Waltham, MA, USA). Images taken with a fluorescence microscope (DM5000B; Leica, Wetzlar, Germany) were merged using Photoshop (Adobe, San Jose, CA, USA).

Mutation analysis

Cancerous and non-cancerous liver tissues of approximate volume of 50 mm^3 were macroscopically dissected, frozen in liquid nitrogen and powdered with a frozen-cell crusher (Cryo-press; Microtec, Funabashi, Japan). Genomic DNA and total RNA were extracted using the QIAamp DNA Mini kit (Qiagen, Duesseldorf, Germany) and the QuickGene kit (Fuji, Tokyo, Japan) from liquid nitrogen-frozen tissues that had been dissected macroscopically from non-cancerous livers and cancerous nodules. Sequencing of *Trp53* was performed as described earlier (Matsumoto *et al.*, 2007) except for primers for the non-transcribed regions, sequences of which are shown in Supplementary Figure 5. Mutations of the *Myc*, *Pten* and *Cdkn2a* genes were analysed as described (Matsumoto *et al.*, 2007) except for primers, sequences of which are shown in Supplementary Figure 5. Statistical significance was assessed by Fisher's exact test using Stata 8.2 software (Stata Corp, College Station, TX, USA). Searching for SHM hot spot motifs and DNA secondary structure analyses were performed using GENETYX-MAC 14 (Genetyx Corp., Tokyo, Japan) and mfold software (Zuker, 2003), respectively.

qRT-PCR

cDNA was synthesized using the iScript kit (Bio-Rad, Hercules, CA, USA). Quantitative PCR (qPCR) was performed using QuantiTect reagent (Qiagen) and a real-time thermal cycler (Mx3000P; Stratagene, La Jolla, CA, USA). Oligonucleotide sequences are shown in Supplementary Figure 5.

Western blotting

Mouse organs were dissected, frozen in liquid nitrogen and powdered with a frozen-cell crusher (Cryo-press). Proteins were extracted from the tissue powder using 10 mM sodium phosphate (pH 6.8), 200 mM NaCl, 1.5 mM $MgCl_2$ and 0.2 mM EDTA with a protease inhibitor cocktail (Complete; Roche Diagnostics, Mannheim, Germany). Protein of 100 μg per lane was applied to a 5–20% polyacrylamide gel (Bio-Rad), electrophoresed and blotted on to Hybond P membrane (GE Healthcare, Buckinghamshire, UK). Signals were generated using peroxidase-labelled anti-rat IgG (Jackson ImmunoResearch) and the ECL Plus system (GE Healthcare) and detected with a LAS-3000 mini image analysis system (Fuji).

Acknowledgements

We thank Dr Andras Nagy for his generous gift of TNAP-Cre mice, Dr Takashi Shinohara for suggesting the choice of the Cre mouse strain, Dr Yoshinobu Toda for the preparation of tissue sections and Dr Masayuki Tsuji for technical help with the immunohistochemical analyses. We also thank Dr Sidonia Fagarasan for critical reading of the manuscript and discussions. This study was supported by Grant-in-Aid for Scientific Research (17013042 and 18390122) and the Takeda Science Foundation.

References

Endo Y, Marusawa H, Kinoshita K, Morisawa T, Sakurai T, Okazaki IM *et al.* (2007). Expression of activation-induced cytidine deaminase in human hepatocytes via NF-kappaB signaling. *Oncogene* **26**: 5587–5595.

Factor VM, Kao CY, Santoni-Rugiu E, Woitach JT, Jensen MR, Thorgeirsson SS. (1997). Constitutive expression of mature transforming growth factor beta1 in the liver accelerates hepatocarcinogenesis in transgenic mice. *Cancer Res* **57**: 2089–2095.

Fan CY, Pan J, Usuda N, Yeldandi AV, Rao MS, Reddy JK. (1998). Steatohepatitis, spontaneous peroxisome proliferation and liver tumors in mice lacking peroxisomal fatty acyl-CoA oxidase. Implications for peroxisome proliferator-activated receptor alpha natural ligand metabolism. *J Biol Chem* **273**: 15639–15645.

Honjo T, Kinoshita K, Muramatsu M. (2002). Molecular mechanism of class switch recombination: linkage with somatic hypermutation. *Annu Rev Immunol* **20**: 165–196.

Horie Y, Suzuki A, Kataoka E, Sasaki T, Hamada K, Sasaki J *et al.* (2004). Hepatocyte-specific Pten deficiency results in steatohepatitis and hepatocellular carcinomas. *J Clin Invest* **113**: 1774–1783.

Katzenellenbogen M, Pappo O, Barash H, Klopstock N, Mizrahi L, Olam D *et al.* (2006). Multiple adaptive mechanisms to chronic liver disease revealed at early stages of liver carcinogenesis in the Mdr2-knockout mice. *Cancer Res* **66**: 4001–4010.

Kim CM, Koike K, Saito I, Miyamura T, Jay G. (1991). HBx gene of hepatitis B virus induces liver cancer in transgenic mice. *Nature* **351**: 317–320.

Kinoshita K, Nonaka T. (2006). The dark side of activation-induced cytidine deaminase: relationship with leukemia and beyond. *Int J Hematol* **83**: 201–207.

Koike K, Moriya K, Iino S, Yotsuyanagi H, Endo Y, Miyamura T *et al.* (1994). High-level expression of hepatitis B virus HBx gene and hepatocarcinogenesis in transgenic mice. *Hepatology* **19**: 810–819.

Koike K, Moriya K, Kimura S. (2002). Role of hepatitis C virus in the development of hepatocellular carcinoma: transgenic approach to viral hepatocarcinogenesis. *J Gastroenterol Hepatol* **17**: 394–400.

Komori J, Marusawa H, Machimoto T, Endo Y, Kinoshita K, Kou T *et al.* (2008). Activation-induced cytidine deaminase links bile duct inflammation to human cholangiocarcinoma. *Hepatology* **47**: 888–896.

Kotani A, Okazaki IM, Muramatsu M, Kinoshita K, Begum NA, Nakajima T *et al.* (2005). A target selection of somatic hypermutations is regulated similarly between T and B cells upon activation-induced cytidine deaminase expression. *Proc Natl Acad Sci USA* **102**: 4506–4511.

Kou T, Marusawa H, Kinoshita K, Endo Y, Okazaki IM, Ueda Y *et al.* (2006). Expression of activation-induced cytidine deaminase in human hepatocytes during hepatocarcinogenesis. *Int J Cancer* **120**: 469–476.

Kues WA, Petersen B, Mysegades W, Carnwath JW, Niemann H. (2005). Isolation of murine and porcine fetal stem cells from somatic tissue. *Biol Reprod* **72**: 1020–1028.

Lomeli H, Ramos-Mejia V, Gertsenstein M, Lobe CG, Nagy A. (2000). Targeted insertion of Cre recombinase into the TNAP gene: excision in primordial germ cells. *Genesis* **26**: 116–117.

Ma W, Xia X, Stafford LJ, Yu C, Wang F, LeSage G *et al.* (2006). Expression of GCIP in transgenic mice decreases susceptibility to chemical hepatocarcinogenesis. *Oncogene* **25**: 4207–4216.

Maeda S, Kamata H, Luo JL, Leffert H, Karin M. (2005). IKKbeta couples hepatocyte death to cytokine-driven compensatory proliferation that promotes chemical hepatocarcinogenesis. *Cell* **121**: 977–990.

Marusawa H. (2008). Aberrant AID expression and human cancer development. *Int J Biochem Cell Biol* **40**: 1399–1402.

Matsumoto Y, Marusawa H, Kinoshita K, Endo Y, Kou T, Morisawa T *et al.* (2007). Helicobacter pylori infection triggers aberrant expression of activation-induced cytidine deaminase in gastric epithelium. *Nat Med* **13**: 470–476.

Morgan HD, Dean W, Coker HA, Reik W, Petersen-Mahrt SK. (2004). Activation-induced cytidine deaminase deaminates 5-methylcytosine in DNA and is expressed in pluripotent tissues: implications for epigenetic reprogramming. *J Biol Chem* **279**: 52353–52360.

Murakami H, Sanderson ND, Nagy P, Marino PA, Merlino G, Thorgeirsson SS. (1993). Transgenic mouse model for synergistic effects of nuclear oncogenes and growth factors in tumorigenesis: interaction of c-myc and transforming growth factor alpha in hepatic oncogenesis. *Cancer Res* **53**: 1719–1723.

Muto T, Okazaki IM, Yamada S, Tanaka Y, Kinoshita K, Muramatsu M *et al.* (2006). Negative regulation of activation-induced cytidine deaminase in B cells. *Proc Natl Acad Sci USA* **103**: 2752–2757.

Nakau M, Miyoshi H, Seldin MF, Imamura M, Oshima M, Taketo MM. (2002). Hepatocellular carcinoma caused by loss of heterozygosity in Lkb1 gene knockout mice. *Cancer Res* **62**: 4549–4553.

Okazaki IM, Hiai H, Kakazu N, Yamada S, Muramatsu M, Kinoshita K *et al.* (2003). Constitutive expression of AID leads to tumorigenesis. *J Exp Med* **197**: 1173–1181.

Petitjean A, Mathe E, Kato S, Ishioka C, Tavtigian SV, Hainaut P *et al.* (2007). Impact of mutant p53 functional properties on TP53 mutation patterns and tumor phenotype: lessons from recent developments in the IARC TP53 database. *Hum Mutat* **28**: 622–629.

Riehle KJ, Campbell JS, McMahan RS, Johnson MM, Beyer RP, Bammler TK *et al.* (2008). Regulation of liver regeneration and hepatocarcinogenesis by suppressor of cytokine signaling 3. *J Exp Med* **205**: 91–103.

Sakurai T, Maeda S, Chang L, Karin M. (2006). Loss of hepatic NF-kappa B activity enhances chemical hepatocarcinogenesis through sustained c-Jun N-terminal kinase 1 activation. *Proc Natl Acad Sci USA* **103**: 10544–10551.

Sandgren EP, Quaife CJ, Pinkert CA, Palmiter RD, Brinster RL. (1989). Oncogene-induced liver neoplasia in transgenic mice. *Oncogene* **4**: 715–724.

Schreck S, Buettner M, Kremmer E, Bogdan M, Herbst H, Niedobitek G. (2006). Activation-induced cytidine deaminase (AID) is expressed in normal spermatogenesis but only infrequently in testicular germ cell tumours. *J Pathol* **210**: 26–31.

Sell S. (2001). Heterogeneity and plasticity of hepatocyte lineage cells. *Hepatology* **33**: 738–750.

Thorgeirsson SS, Grisham JW. (2002). Molecular pathogenesis of human hepatocellular carcinoma. *Nat Genet* **31**: 339–346.

Tsuji M, Suzuki K, Kitamura H, Maruya M, Kinoshita K, Ivanov II *et al.* (2008). Requirement for lymphoid tissue-inducer cells in isolated follicle formation and T cell-independent immunoglobulin a generation in the gut. *Immunity* **29**: 261–271.

Urven LE, Weng DE, Schumaker AL, Gearhart JD, McCarrey JR. (1993). Differential gene expression in fetal mouse germ cells. *Biol Reprod* **48**: 564–574.

Vogelstein B, Kinzler KW. (2004). Cancer genes and the pathways they control. *Nat Med* **10**: 789–799.

Wang L, Duan E, Sung LY, Jeong BS, Yang X, Tian XC. (2005). Generation and characterization of pluripotent stem cells from cloned bovine embryos. *Biol Reprod* **73**: 149–155.

Yoshikawa K, Okazaki IM, Eto T, Kinoshita K, Muramatsu M, Nagaoka H *et al.* (2002). AID enzyme-induced hypermutation in an actively transcribed gene in fibroblasts. *Science* **296**: 2033–2036.

Zuker M. (2003). Mfold web server for nucleic acid folding and hybridization prediction. *Nucleic Acids Res* **31**: 3406–3415.

Supplementary Information accompanies the paper on the Oncogene website (http://www.nature.com/onc)